Analytical Biochemistry **291,** 175–197 (2001)
doi:10.1006/abio.2000.5006, available online at http://www.idealibrary.com on IDEAL®

REVIEW

Seeing the Wood through the Trees: A Review of Techniques for Distinguishing Green Fluorescent Protein from Endogenous Autofluorescence


Nicholas Billinton


Andrew W. Knight

Nicholas Billinton* and Andrew W. Knight†,[1]

**Department of Biomolecular Sciences and †Department of Instrumentation and Analytical Science, University of Manchester Institute of Science and Technology, P.O. Box 88, Manchester M60 1QD, United Kingdom*

Published online March 16, 2001

The green fluorescent protein (GFP)[2] from the jellyfish *Aequorea victoria* has recently leapt to prominence within numerous biological fields. Interest in the use of GFP has grown enormously over the past 5 years. The number of papers concerning GFP held in the Web of Science database, which abstracts the scientific literature (http://wos.mimas.ac.uk), rose from 13 in the period 1981–1994, to over 3400 in the period 1995 to October 2000. This is due to the ability to clone and heterologously express GFP genes in a diverse range of cells and organisms, from bacteria and yeast, to plants and mammals, coupled with favorable properties such as high stability, minimal toxicity, noninvasive detection, and the ability to generate the highly visible fluorophore *in vivo* in the absence of external cofactors. Thus, GFP has become a truly versatile marker for visualizing physiological processes, monitoring subcellular protein localization, distinguishing successful transfection, or reporting on gene expression. As such a powerful tool, GFP now impinges on almost every area of biological research.

However, unless GFP is very highly expressed or densely localized, the fluorescence signal from GFP will invariably be contaminated with endogenous cellular or media fluorescence. Researchers often think they have failed in effectively using GFP as a marker, when actually they have succeeded. Their real problem was simply the detection of GFP in the sea of other fluorescent species within biological material, which fluoresce at a similar wavelength. Cells in most organisms exhibit a natural fluorescence, commonly called "autofluorescence," from a range of species including metabolites and structural components. This has been characterized in such diverse examples as human epidermal cells (1), rat hepatocytes (2), *Drosophila melanogaster* (3), numerous fungi (4–6), and plants such as maize (7) and alfalfa (8). Many cellular metabolites exhibit autofluorescence, and since cellular extracts are often crucial components of culture media, such media can also be intensely autofluorescent, compounding the problem.

Autofluorescence spectra are generally broad and encompass most of the visible spectral range, overlapping the emission wavelengths of green fluorescent protein and its many derivatives. When measuring GFP, the presence of autofluorescence often leads to

[1] To whom correspondence and reprint requests should be addressed. Fax: 44-161-200-4911. E-mail: a.knight@umist.ac.uk.

[2] Abbreviations used: GFP, green fluorescent protein; FMN, flavin mononucleotide; FAD, flavin adenine dinucleotide; AGEs, advanced glycation end-products; FFI, 2-(2-furoyl)-4(5)-(furanyl)-1*H*-imidazole; BFPs, blue fluorescent proteins; FITC, fluorescein isothiocyanate; LED, light emitting diode; CCD, charge coupled devices; PMT, photomultiplier tubes; RGB, red–green–blue; CLSM, confocal laser scanning microscopy; TPLSM, two-photon laser scanning microscopy; FLIM, fluorescence lifetime imaging microscopy; CE, capillary electrophoresis; LB, Luria-Bertani; FRET, fluorescence resonance energy transfer; CFP, cyan fluorescent protein; YFP, yellow fluorescent protein; yEGFP, yeast-enhanced GFP.

0003-2697/01 $35.00

low signal-to-noise ratios, restriction of detection sensitivity, and in some cases even failure to detect or visualize GFP at all. Autofluorescence also reduces the contrast and clarity of GFP labeled structures in fluorescence microscope images.

This paper will first review the current opinion on the source, chemical nature, and spectroscopic characteristics of autofluorescent molecules across a wide range of species. Then, for the first time, the various methods open to the researcher to overcome the problems of GFP determination in the presence of autofluorescence will be systematically and critically reviewed. The methods discussed all contribute to sensitive detection, accurate localization, or sharp visualization of GFP.

The discussion will include instrumentation approaches that exploit differences between GFP and autofluorescent species in terms of their fluorescence emission wavelength, bandwidth, anisotropy, and lifetime. Alternatively, chromatographic and other separation techniques are included which rely on differences in chemical and physical properties. Also covered are microscopy methods used to specifically target localized GFP while discriminating against autofluorescent structures and organelles. In addition, software methods which can be used to remove autofluorescence and enhance GFP visualization in fluorescence microscope images are considered.

Chemical methods for reducing autofluorescence include the careful selection of growth media and pH, and the use of colored dyes which specifically quench autofluorescence. Photochemical methods include photobleaching, photoconversion of GFP to produce alternative fluorescence wavelengths, and the use of fluorescence resonance energy transfer. Finally, biochemical methods for GFP signal enhancement cover the use of more active promoters, and the choice of GFP mutants to give brighter fluorescence or alternative emission wavelengths.

It is hoped that by gaining greater insight into the sources of autofluorescence, and making use of one or more of the variety of autofluorescence discrimination methods discussed, the researcher will be able to "see the wood through the trees."

POTENTIAL BIOCHEMICAL SOURCES OF AUTOFLUORESCENCE

Flavins

Flavins are ubiquitous coenzymatic redox carriers in the metabolism of most organisms and as photoreceptors in plants and fungi. Flavin mononucleotide (FMN) and flavin adenine dinucleotide (FAD) are the most common flavins and are derivatives of riboflavin (vitamin B_2). FMN and riboflavin are the most intensely fluorescent flavins, with maximal emission at 530 nm, while FAD is about 10 times less fluorescent. As long ago as the 1940s, these properties were being exploited in the quantification of flavins. In a study of vitamin content in the malpighian tubes of *Periplaneta americana* (American roach), the presence of riboflavin was ascertained and quantified by its "yellow–green" fluorescence (9).

Two early studies to identify the sources of intracellular autofluorescence provided further important evidence that flavoproteins are a major cause. In the first, excitation of various cells with blue light (488 nm) resulted in emission spectra with a fluorescence peak between 540 and 560 nm (10). This corresponds to the fluorescence characteristics of flavoproteins which are typically 10–30 nm red-shifted with respect to the free flavin. The second study analyzed the fluorescence of viable mammalian cells and revealed broad excitation maxima centered around 380 and 460 nm with maximal emission at 520 nm. This was suggested to arise from intracellular riboflavin, flavin coenzymes, and flavoproteins in the mitochondria (11).

Cumulative evidence confirms that flavins excited with blue light (450–490 nm) fluoresce with a green–yellow color (500–560 nm), spectroscopic characteristics not dissimilar to those of GFP. Table 1 lists examples of autofluorescent cellular components. This list demonstrates the broad range of cell types exhibiting such fluorescence, along with their spectral properties.

NAD(P)H

Nicotinamide-adenine dinucleotide (NAD^+/NADH) and nicotinamide-adenine dinucleotide phosphate ($NADP^+$/NADPH), like FAD and FMN, are fluorescent coenzymes crucial to many reactions in most cell types. Since both NAD^+ and $NADP^+$ have equal standard reduction potentials, they shall be referred to as NAD(P)H. The report of van Duijn on examples of primary fluorescence for users of fluorescence microscopy (12) quotes nicotinamide as exhibiting "bluish-white" fluorescence in the free state, but green fluorescence when observed in the reticuloendothelial system of phagocytic cells, responsible for the degradation of foreign bodies and material. The blue fluorescence is dependent on the redox state and environment of the coenzyme. It must be in the reduced state to exhibit fluorescence. Binding to protein cofactors results in enhancement of fluorescence intensity and/or alters the wavelength of maximal emission, resulting in a blue-shift (13). Maximal excitation of free NAD(P)H occurs at ~360 nm with emission at ~460 nm, and there is a ~20 nm blue-shift for the protein-bound coenzyme (440 nm). These properties were shown to hold true for baker's yeast (*Saccharomyces cerevisiae*), rat liver cells, and Chinese hamster ovary (CHO) cells (11, 13).

TABLE 1

Common Biochemical Sources of Autofluorescence in a Wide Variety of Cell Types and Organisms, with Their Respective Emission and Excitation Maxima as Reported in the References Given

Autofluorescent source	Organism/tissue	Emission wavelength/nm	Excitation wavelength/nm	Reference
Flavins	CHO cells	520	380, 460	(11)
	Rat hepatocytes	525	468	(2)
	Bovine and rat neural cells	540–560	488	(10)
	Goldfish inner ear	540	450	(61)
	Periplaneta americana	"Yellow–green"	UV	(9)
NAD(P)H	Rat cardiomyocytes	~509	~395	(114)
	S. cerevisiae, rat hepatocytes	440–470	366	(13, 14)
	CHO cells	440–450	360	(11)
Lipofuscins	Rhesus monkey, rat, human medulla	"green"	460–490	(20)
	Rat heart	550	450–490	(19)
	Muscle, myocardium, hepatocytes	~540–560	360	(18)
	Human brain	481–673	435	(115)
	Rat liver	430	345	(116)
	Rat retina	>510	390–490	(117)
AGEs	Chinese hamster and human lenses	434	365	(24)
	In vitro	440–450	370	(22)
	Human cornea	385	320	(23)
	Diabetic human skin	440	365	(25)
Collagen and elastin	Human aorta and coronary artery	>515	476	(26)
	Human skin	470–520	442	(27)
Protoporphyrin IX	Human psoriatic skin	635	442	(27)
Lignin	*Phyllostachys pubescens*	UV	470–510	(29)
	Pinus radiata	488	~530	(30)
Chlorophyll	Green algae thylakoid	488	685 (740)	(31)

Two independent studies of cellular autofluorescence in viable mammalian cells (11) and *S. cerevisiae* (14) led to the conclusion that cellular fluorescence could be divided into two parts: (i) excitation at 365 nm with emission at 445 nm, and (ii) excitation maxima at 380 and 440 nm with emission at 520 nm. After comparison with contemporary literature on the fluorescence properties of known metabolites, these were seen to be representative of NAD(P)H and flavins, principally riboflavin, respectively. It is also worth noting that the fluorescence intensity due to NAD(P)H was between 50 and 100 times that due to flavins (11).

Thus far, autofluorescent sources affecting green- and blue-emitting fluorescent proteins have been considered. However, the broad spectral diversity now available from the ever-expanding range of GFP mutants means that sources of background fluorescence other than green-emitters must be considered. A selection of such potential sources is briefly discussed below.

Lipofuscins

The term "lipofuscin" refers to a dark lipopigment that emits orange–yellow fluorescence. It is something of an enigmatic substance, found to positively stain for lipid, carbohydrate, and protein, though inconsistently between different cell types and in the hands of different researchers. Lipofuscin is also called "age pigment" since its strong autofluorescence is seen more frequently with increasing age, in the cytoplasm of postmitotic cells (reviewed in 15). It has been found in cells from a wide range of species and appears as irregular yellow–brown granules of 1–20 μm diameter. These granules almost invariably have single membrane envelopes.

Lipofuscinogenesis (lipofuscin formation) is age-related and may result from the gradual failure of the cell's recycling systems (reviewed in 16). Material damaged by continual exposure to oxidative and free radical attack accumulates, reacting and cross-linking to form large, heterogeneous fluorescent complexes. The fluorescence properties of lipofuscin appear to be subject to differences of opinion but most studies agree that maximal excitation of lipofuscin fluorescence occurs at near-visible ultraviolet wavelengths (330–390 nm). Autofluorescent emission can vary from blue (420 nm) (17) to an orange–yellow in color (540–560 nm) (18), or encompass a wide spectral range (450–650 nm). In a study of the relationship between lipofusci-

nogenesis and glutathione concentration, cultured rat cardiomyocytes fluoresced at 550 nm when excited at 450–490 nm (19). These wavelengths are sufficiently close to those of GFP to cause spectral overlap and hence interference. Furthermore, fluorescence microscopy of human, monkey, and rat neural tissues demonstrated green fluorescence from lipofuscin-like autofluorescent pigments, using optical filters for fluorescein (20), which has almost identical spectroscopic properties to the commonly used S65T GFP and other enhanced derivatives.

AGEs

AGEs are advanced glycation end-products, where glycation refers to nonenzymatic glycosylation, also known as the Maillard reaction. These reactions consist of the addition of an aldehyde sugar to an amino group, resulting in condensation products known as Amadori products. Amadori products can undergo subsequent rearrangements and reactions to form structurally diverse complexes that are called AGEs. These are better characterized than lipofuscins, the term AGE representing a large family of mostly nitrogenous, cyclic, and conjugated complexes or polymers that may be free or bound to proteins or other macromolecules.

Several AGEs have been chemically identified. An example is 2-(2-furoyl)-4(5)-(furanyl)-1*H*-imidazole (FFI) (21), which is autofluorescent and has a fluorescence spectrum [excitation at 370 nm and emission at 440–450 nm (22)] similar to that of aged eye lens proteins and collagen. Because of the involvement of sugars (primarily glucose) in advanced Maillard reactions, AGEs are associated with disease states such as diabetes mellitus. Changes in the cornea of the eye are associated with diabetes, and these include increased corneal autofluorescence. Modification of collagen by AGEs is implicated in this increased fluorescence (320 nm excitation and 385 nm emission) (23). A more recent study, utilizing more AGE-appropriate wavelengths and filter sets, also demonstrated that diabetic lenses (hamster and human) are more fluorescent than nondiseased lenses, with a peak excitation of 365 nm and emission at 434 nm (24). The diabetes link was further shown when pentosidine, an AGE, was found at elevated levels in the skin collagen of long-term diabetes patients, coinciding with increased fluorescence (370 nm excitation and 440 nm emission) (25).

Autofluorescence from AGEs is most significant in the measurement of blue-shifted derivatives of GFP, the so-called blue fluorescent proteins (BFPs) and Clontech's GFPuv (see Table 3). The BFPs exhibit much lower quantum yields than their green counterparts, resulting in relatively poor signal-to-noise ratios.

Elastin and Collagen

Autofluorescence of structural components in animals has already been mentioned in relation to the role of collagen in AGE formation in disease and aging. However, structural proteins like collagen and elastin have further autofluorescence properties. A study of laser-excited autofluorescence in the aorta and the coronary artery of humans revealed green–yellow fluorescence from collagen and elastin fibers with excitation at 476 nm (26).

Protoporphyrin IX

Another study on human skin revealed autofluorescence at wavelengths similar to those for GFP (27). The skin of psoriatic patients was examined spectrofluorometrically, revealing that normal skin showed a broad peak of fluorescence emission between 470 and 520 nm (excitation at 442 nm). This clearly corresponds with the peak emission from such GFPs as the S65T derivative and the EGFP, and is presumably a result of the elastin and collagen autofluorescence discussed above. However, while psoriatic skin from the same patients showed the same blue–green broad emission, there was a further distinct peak of emission at 635 nm. The extra peak in the disease state was shown to be caused by increased levels of protoporphyrin IX, which is an intermediate in the biosynthetic pathway for heme. While 635 nm is a significantly longer wavelength than that at which the traditional GFPs emit (~510–520 nm), a red fluorescent protein was recently discovered (28). The red fluorescent protein, now marketed by Clontech as DsRed, has the most red-shifted spectral properties of the known fluorescent proteins, with maximal excitation at 558 nm and emission at 583 nm (see Fig. 8). Red autofluorescent sources such as protoporphyrin IX are likely to be important background components in the measurement of DsRed fluorescence.

Lignin

Plants have other autofluorescence problems that are disruptive to GFP detection. Of course, the obvious problem is the reflection of visible green light by plants (see chlorophyll section below), ensuring that detection of GFP fluorescence in weakly expressed systems is very difficult. However, another problem is lignin, the chief component of woody tissue, which has an associated blue autofluorescence. Attempted detection of GFP fluorescence in transgenic maize plants revealed blue background autofluorescence that appeared to be less intense in younger leaves (7). This was suggested to be due to the lower lignin content of the cell walls in younger samples. However, the blue autofluorescence can appear green depending upon the environment of the sample. For example, in work with bamboo, UV

excitation resulted in blue fluorescence until samples were treated with ammonia, when fluorescence intensity increased and changed color to green (the peak shifting from 470 nm to 510 nm) (29). Another study, on *Pinus radiata* mild compression wood, directly demonstrated green fluorescence from lignified tissue after illumination at 488 nm (argon-ion laser) and with imaging at 530 nm (30), although the authors suggest that there may have been significant contribution from holocellulose at these wavelengths. These two studies indicate the spectral changes that can occur by manipulating the sample environment.

Chlorophyll

Chlorophyll (in particular types *a* and *b*) is the most abundant of the photosynthetic chromophores and is related to protoporphyrin IX of hemoglobin and myoglobin. Both chlorophylls *a* and *b* absorb strongly in the deep blue and red regions of the visible spectrum and thus green light that is reflected back from the plant tissue can mask GFP fluorescence. However, chlorophyll is also autofluorescent with maximal excitation at 488 nm and maximal emission at 685 nm with a broad shoulder at 740 nm (31). In an early study to use GFP as a vital marker in plants, the *Aequorea* GFP was utilized as a marker for gene expression and for FACS analysis in *Arabidopsis* (32). Bright green fluorescence from GFP was detectable in ~50% of transfected cells, even in the presence of blue autofluorescence from the vacuole and red autofluorescence from the chloroplasts. However, overlap of GFP fluorescence and red chlorophyll autofluorescence resulted in patches of bright yellow fluorescence. Stewart makes the point in a discussion on monitoring transgenic plants using GFP that GFP expression must be high enough to mask the red fluorescence from chlorophyll (33).

Drosophila

Drosophila warrants a special mention since Plautz and Kay (3, 34) cite autofluorescence as the greatest difficulty encountered using GFP in the fly. When excited at GFP wavelengths, the cuticle of the fly exhibits a yellow fluorescence with a peak separated by 50 nm from that of GFP. Fluorescence from yolk in vitellogenic and mature oocytes, and young embryos, can also make GFP fluorescence difficult to detect (35, 36).

Media Components and Related Molecules

Only aromatic amino acids exhibit significant autofluorescence. Tryptophan fluoresces with the greatest quantum yield, with maximal excitation at 287 nm and emission centered at 348 nm. Tyrosine and phenylalanine are less fluorescent with excitation at 275 and 260 nm and emission centered at 303 and 282 nm, respectively. The tyrosine derivatives, adrenaline and noradrenaline, exhibit spectral properties significantly red-shifted from tyrosine. Adrenaline is excited at 330 and 420 nm and exhibits fluorescence at 525 nm, while noradrenaline is excited at 325 and 395 nm with maximal emission at 515 nm. These are potentially important for GFP detection in human tissues. In addition, melatonin is a derivative of tryptophan and is excited at 300 nm with emission at 540 nm, which may interfere with the detection of red-shifted GFP mutants. Histidine is not naturally fluorescent although its imidazole ring is reactive and can form fluorescent products. For example, L-histidine can react with *N*-bromosuccinimide to produce a species that is maximally excited at 400 nm and exhibits fluorescence at 520 nm (37).

TABLE 2

Selected Autofluorescent Vitamins and Their Spectral Characteristics (37)

Vitamin	Emission wavelength/nm	Excitation wavelength/nm
Pyridoxine	350–400	300–340
Ascorbic acid	430	350
Nicotinamide	460	360
Vitamin D	470	390
Vitamin A	490	340
Riboflavin	500–560	450–490

The adenine biosynthesis mutants in budding yeast, *ade1* and *ade2*, appear pink under normal room lighting, due to the accumulation of a metabolic intermediate (phosphoribosylaminoimidazole). This pigment interferes with GFP detection under FITC filter conditions, since the pink cells appear bright yellow or green (38). Addition of supplementary adenine to the growth medium reduces the autofluorescent interference, although *ade* strains should be avoided where possible.

Finally a number of vitamins are autofluorescent due to their delocalized ring structures. Table 2 illustrates selected examples of autofluorescent vitamins and their spectral properties. Environmental conditions can significantly alter the spectral properties detailed here. However, these effects are beyond the scope of this review and have been discussed elsewhere (37).

INSTRUMENTATION METHODS FOR AUTOFLUORESCENCE DISCRIMINATION

Optimized Filter Sets

In the majority of spectroscopic techniques that have been used to visualize or quantify GFP expressed in

cells and organisms, carefully selected optical filters have been employed to discriminate between GFP and naturally occurring autofluorescence. Ideally such filters pick out areas of the spectrum such that GFP can be excited, and its fluorescence transmitted, with greater efficiency than the autofluorescent species. Due to the remarkably similar spectral characteristics of fluorescein and common GFP variants, some workers have been able to simply use the widely available filter sets for the fluorescent probe fluorescein isothiocyanate (FITC), fitted to most fluorescence microscopes. The FITC filter set is suitable for viewing the commonly used blue excitation enhanced GFPs, such as S65T and its derivatives, while UV filter sets can be used for viewing wild-type and UV-shifted GFPs such as the BFPs. However, in general, this approach is only successful in cases where the GFP to autofluorescence ratio is high, for example by the use of a highly expressed, densely localized or especially bright GFP mutant. Since the excitation and emission peaks of autofluorescent components invariably overlap or lie very close to those of GFP, standard FITC filter sets are often not specific enough to adequately discriminate GFP from autofluorescence.

A typical fluorescence filter set will consist of an excitation filter, a dichroic beamsplitter, and an emission filter. In a fluorescence microscope these three components are generally combined in a "filter cube" or "block." Other instrumentation uses similar filters in various orientations; however, the selection criteria will be broadly similar. Filter sets dedicated to GFP applications have recently been made commercially available. These can be tailored in size to suit most microscopes and filter holders; however, they are relatively expensive, costing several hundred pounds per set. Suppliers such as Chroma Technology Corp. and Omega Optical Inc. (both Brattleboro, VT) market over 30 different filter sets for GFP, each dedicated to a particular GFP variant or to overcome a specific autofluorescence problem. This diversity highlights the reasons why most researchers have chosen to optimize their own filter sets, often from a combination of different suppliers (39): first, because the autofluorescence arises from a disparate, and often unknown, range of molecules, which vary enormously between different cells and species and hence is specific to a given application; and second, because new genetically engineered GFP mutants with diverse spectroscopic properties are constantly being developed.

The choice of excitation filter is dependent primarily on the light source used and the excitation characteristics of the selected GFP, as well as more specific autofluorescence considerations. Several common light sources are employed for GFP excitation. The mercury arc lamp produces a series of useful lines between 400 and 500 nm, whereas the xenon arc lamp and halogen lamp produce a relatively broad continuous spectrum in the visible range. For all of these sources a fairly broad bandpass excitation filter would be the one of choice to allow sufficient light transmission for efficient GFP excitation, such as a 475/40 with transmission in the range 455 to 495 nm. However, for many specimens the use of a broad bandpass filter may lead to a reduction in overall signal-to-noise ratio, since the increase in autofluorescence will outweigh the increase in the GFP fluorescence signal. In this case, narrower band excitation filters may be more usefully employed such as a 475/20. Excitation of GFP with the intense blue laser line of the argon ion laser (488 nm), allows the use of very narrow excitation filters, such as 488/10 or 488/3 interference filters. This combination limits the autofluorescence to that which arises only from those species whose excitation spectra significantly overlap the excitation peak of GFP.

Randers-Eichhorn *et al.* reported a filter set used for excitation of GFP in *Escherichia coli* using a bright blue light-emitting diode (LED) (40). The brightest blue LEDs manufactured by the Nichia Corporation of Japan, have a luminous intensity of 2000 m cd, centered at 470 nm and extending from 430 to 510 nm. The relatively wide bandwidth of the LED emission can cause interference problems and is best used with a relatively narrow bandpass excitation filter, Randers-Eichhorn *et al.* employing a 458/10 interference filter.

The choice of emission filter is dependent primarily on the type of detector employed and the emission characteristics of the GFP used. Common detectors include the eye, charge coupled devices (CCD), video cameras, photographic film and photomultiplier tubes (PMT). Depending on the application in question, either a bandpass or long-pass emission filter is used. For more qualitative applications where GFP is visualized using the eye or detectors capable of recording color images, long-pass filters may be used because the sharp bright green of GFP may be distinguished from the broad spectrum autofluorescence (3). In cases where only intensity and no color data is recorded, such as with a PMT or monochrome camera, then narrow bandpass filters are employed to distinguish between GFP and autofluorescence, such as a 510/20 interference filter. This is especially the case when quantitative data is required, such as in fluorimetric or flow cytometric methods.

Further optimization of standard filter sets may simply be made by the addition of extra long-pass or bandpass filters. However, as a significant proportion of the available fluorescence is lost with each additional filter, typically 10 to 30%, sensitivity will be further reduced. In addition, further fluorescence signal may be lost in the process of collimating the light, since most interference and bandpass filters effectively dis-

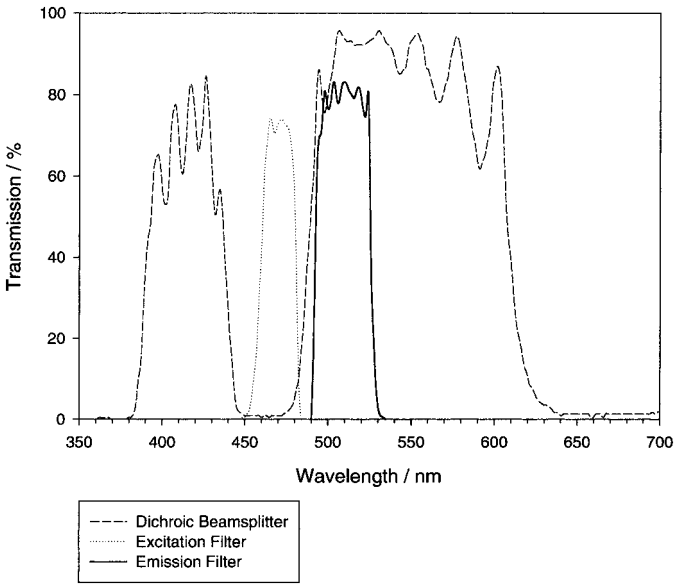

FIG. 1. Transmission spectra of Omega Optical Incorporated GFP filter set XF116, specifically designed for researchers experiencing high autofluorescence. Adapted from company literature with permission of Omega Optical Inc. (Brattleboro, VT).

criminate wavelength for only light striking the filter at 90° to their surface.

Finally the choice of dichroic beamsplitter used in microscope filter cubes depends entirely on spectral properties of the chosen excitation and emission filters. The dichroic filter is placed at a 45° angle to the incoming excitation light, and should ideally reflect greater than 90% of the excitation light toward the sample, while transmitting more than 90% of the fluorescence back to the microscope eyepiece or photodetector. The cutoff wavelength of the dichroic filter should fall between the transmission windows of the excitation and emission filters thus eliminating cross-talk interference, and is typically in the range 490–505 nm for GFP.

A diagram of the spectral characteristics of a commercial filter set designed especially for researchers having problems with autofluorescence swamping their GFP signal is shown in Fig. 1. The use of narrower band filters, in this example to restrict excitation and emission wavelengths, leads however to a much dimmer image than the standard GFP filter set, and is therefore only recommended where autofluorescence is a particular problem, such as in plant research. A discussion of useful filter sets for GFP and a selection of protocols for the visualization of GFP using various instruments and in specific cells and organisms has been documented by Endow and Piston (41).

While it is imperative to optimize the filter set for GFP visualization, the quality of the other elements of the microscope should not be neglected. High-quality objective lenses, internal prisms, light transducers, and other components should be used where possible, so as not to introduce light which may be perceived as an erroneous fluorescence signal, or which may obscure the fluorescence signal being measured.

Dual-Wavelength Differential Fluorescence Correction

Dual-wavelength differential fluorescence correction methods exploit the fact that autofluorescence excitation and emission spectra are generally broad with few features, extending over several hundred nanometers, whereas the excitation and emission spectra of the target fluorophore, such as GFP, are relatively narrow and well-defined stretching over typically 50 to 100 nm. There are two main approaches in this technique: (i) the use of two excitation wavelengths with fluorescence measurement at a single wavelength, and (ii) the use of a single excitation wavelength with fluorescence measurement at two wavelengths.

Steinkamp and Stewart reported a method for reducing background autofluorescence in flow cytometry using different lasers to provide two excitation wavelengths; however, the principles could be applied to many other experimental methods and instruments (42). Although based on FITC, the method should also be suitable for GFP. An argon-ion laser line (488 nm) was used to optimally excite the fluorophore plus the autofluorescent components of the cell, while a krypton laser line (413 nm) was used to principally excite only the autofluorescence. The fluorescence readings that result from excitation by each laser respectively are measured in the same wavelength region, and subtracted on a cell by cell basis, using a differential amplifier to zero the autofluorescence and amplify the remaining signal from the fluorophore.

In the flow-cytometric method the two laser beams were physically spaced 250 μm apart, such that the cell passed first through one laser beam and then through the second, giving two distinct fluorescence pulse signals. Alternatively, a fixed sample could be illuminated first with one laser light source and then the other to obtain the two separate fluorescence measurements. The method assumes that autofluorescence excitation is nearly uniform between the two laser wavelengths. This is often the case since several species with overlapping fluorescence spectra contribute toward the autofluorescence signal. If however this is not the case, then the input signal amplitudes can be adjusted to balance the differential amplifier output to zero using autofluorescent unlabeled control cells. Figure 2 illustrates the principle of the technique.

One advantage of this technique is that as long as the two lasers are exciting the same autofluorescent chromophores in the cell, the correction method will automatically compensate for factors affecting fluores-

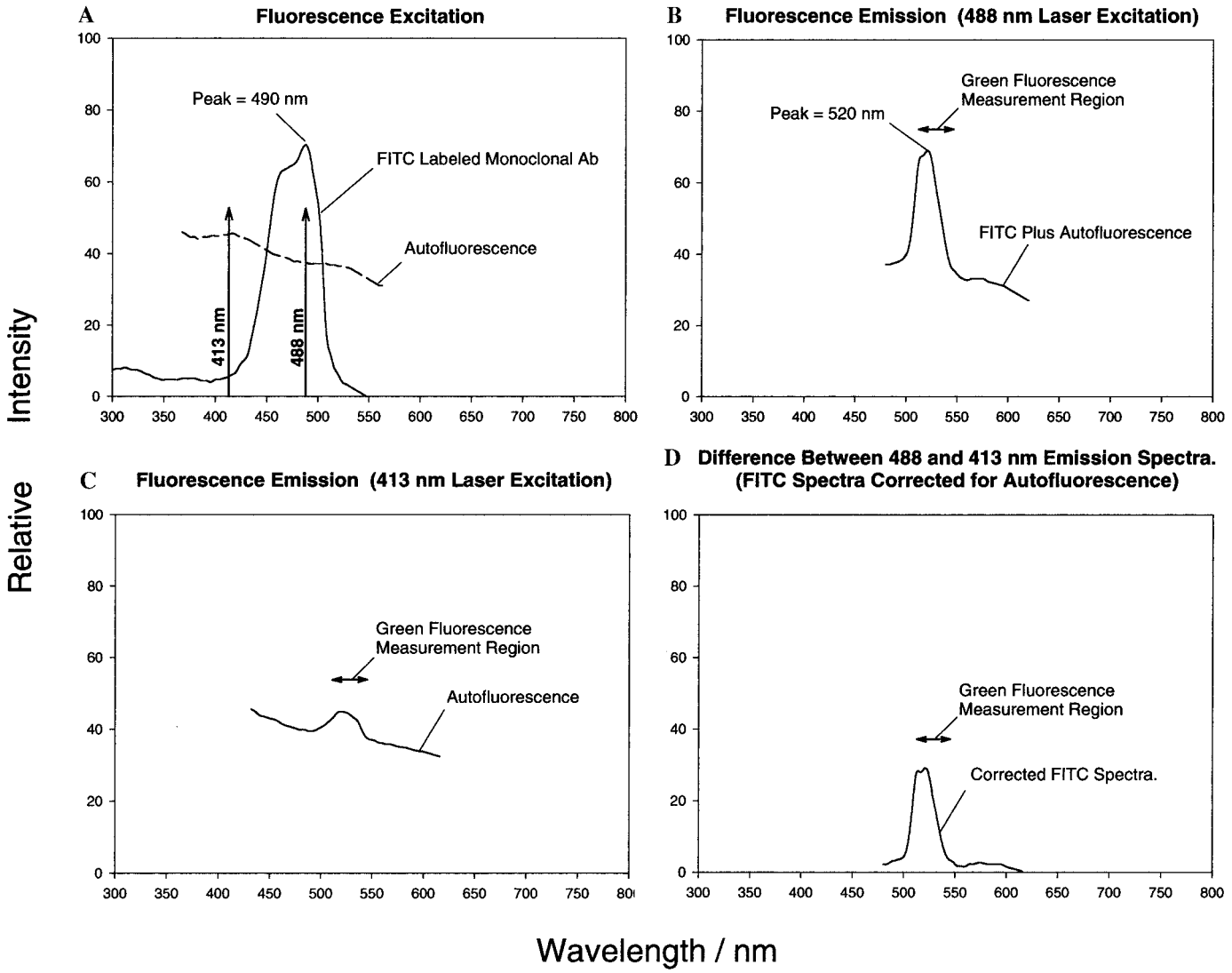

FIG. 2. Conceptual diagram for illustrating (A) fluorescence excitation spectra of fluorescein isothiocyanate (FITC) and clone 9 cell autofluorescence and the 488- and 413-nm laser excitation wavelengths, (B) fluorescence emission of FITC plus autofluorescence for 488 nm excitation, (C) fluorescence emission of autofluorescence for 413-nm laser excitation, and (D) the mathematically calculated difference between the fluorescence emission spectra from 488 and 413 nm, i.e., the emission spectra for FITC corrected for autofluorescence. Green fluorescence measurement region, 515–545 nm. Adapted from Ref. 42, reprinted with permission of Wiley–Liss Inc., a subsidiary of John Wiley & Sons, Inc.

cence in general, such as fluctuations in temperature or pH. In addition, in flow cytometry the correction can be made on a cell by cell basis, so a mixture of high and low autofluorescent cells can be analyzed together. The main disadvantage is the need for an additional narrow band light source focused to excite the same area of the sample, which increases the cost and complexity of existing instrumentation. Additional fast processing electronics are also required for flow-cytometric applications.

These disadvantages are overcome in the converse dual wavelength correction method whereby a single excitation light source is used, and two different emission or other wavelength parameters are measured. Roederer and Murphy explored this approach, again for FITC analysis in flow cytometry, but in such a way as to be applicable for GFP and in a wide range of instrumental formats (43). Excitation of both the fluorophore and autofluorescence was via a single argon-ion laser line (488 nm). The fluorescence of the fluorophore, plus that of the interfering autofluorescent components of the cell, was measured at the optimum 530 nm. This measurement was then mathematically corrected using software by subtracting the autofluorescence component of the signal, which was calculated by correlation to the emission intensity at 625 nm.

Again this method assumes a broad autofluorescence emission against a narrow emission from the target fluorophore, which shows very low intensity at the second wavelength. The method also assumes that the light detector responds with equal sensitivity to the two fluorescence wavelengths selected. Yet if this is not the case, software parameters can be adjusted to compensate using data from unlabeled control cells. Interestingly, the interfering autofluorescent component of the analytical signal, measured at 530 nm, can be estimated from a variety of alternative parameters, provided that they are highly correlated with the autofluorescence of unlabeled control cells, and are not significantly affected by the fluorescence of the probe itself. Roederer and Murphy found a reasonable correlation between side-scattered excitation light at 90° and the autofluorescence intensity. This is assumably due to a relatively constant cytoplasmic concentration of autofluorescent cell constituents, and thus autofluorescence is directly proportional to cell volume and thus size.

Fluorescence Polarization

A method of discriminating GFP from autofluorescence based on the observation that GFP produces significantly polarized fluorescence when excited with plane polarized light has been recently reported by the authors (44, 45). When a sample containing small fluorescent molecules is illuminated with plane polarized light, those molecules with their electronic transition moment aligned parallel to the electric vector of the excitation light are excited. The subsequent fluorescence emission will be largely unpolarized, however, since the molecules are free to rotate during the time taken for the electronic transitions of fluorescence to occur. That is to say their rotational correlation time is much shorter than their fluorescence lifetime, and their molecular orientation effectively becomes randomized before emission occurs. However, since GFP is a relatively large molecule (27 kDa) and the actual fluorophore element is rigidly encapsulated within the cylindrical structure, it rotates in solution at a slow rate compared to its fluorescence lifetime. Swaminathan *et al.* determined the fluorescence lifetime of GFP to be 2.9 and 2.6 ns in aqueous solution and cell cytoplasm, respectively, an order of magnitude faster than the corresponding rotational correlation times of 20 and 36 ns (46). By contrast, fluorescein had a rotational correlation time of 120 ps, 40 times shorter than its fluorescence lifetime.

It was found that when GFP, either in free solution or within whole yeast cells, was excited with plane polarized light from an argon-ion laser, the fluorescence intensity perpendicularly polarized with respect to the laser light source ($I_{\perp}$) was only approximately 50% of that aligned parallel, with respect to the laser light source ($I_{||}$). In contrast, for fluorescein, the fluorescence intensities measured parallel and perpendicular with respect to the polarization of the laser light source were approximately equal. Thus the degree of polarization (P), defined as $(I_{||} - I_{\perp})/(I_{||} + I_{\perp})$, was measured as 0.398 for GFP and 0.004 for fluorescein (45).

It was speculated in this work that autofluorescence in whole cells and conditioned media may contain a significant contribution from smaller fluorescent species, such as flavins and NAD(P)H, which would exhibit low fluorescence polarization. To discriminate between GFP and autofluorescence, the measured fluorescence signal is the difference between $I_{||}$ and $I_{\perp}$, which will be large for GFP, much lower for smaller autofluorescent species, and approximately zero for other small green fluorophores such as fluorescein. The method was successfully applied to improving the quantification of GFP expressed in naturally autofluorescent transgenic yeast strains (45).

Although dedicated fluorescence polarization spectrometers are commercially available, it is relatively easy to adapt existing instrumentation to obtain fluorescence polarization measurements. There are several instrument configurations that can be adopted. Using a single fluorescence detector placed behind a polarizing filter, the plane of polarization of the light source can be switched between two orthogonal planes to enable $I_{||}$ and $I_{\perp}$ measurements to be made. Adjustment of the plane of polarization may be made by use of a rotating polarizing filter or a polarizing beamsplitter. Similarly, the polarization of the light source can be fixed and polarization of light transmitted to the fluorescence detector may be selected to record $I_{||}$ and $I_{\perp}$. Thus a conventional fluorescence spectrometer can be readily adapted simply by slotting inexpensive polarizing filters either side of the cuvette or sample holder and rotating one through 90° between measurements. A more robust arrangement which involves no moving parts is shown in Fig. 3 incorporating a fluorescence flow cell. Two detectors are used, both at right angles to the path of the laser light source. Using fixed polarizing filters, detectors 1 and 2 simultaneously measure $I_{||}$ and $I_{\perp}$, respectively. Once assembled the sensitivity of the two detectors is equalized (electronically or using software) such that $I_{||} = I_{\perp}$ and $P = 0$, using the fluorescence of 8-hydroxypyrene-1,3,6-trisulfonic acid trisodium salt, which has fluorescence characteristics very similar to S65T GFP, while demonstrating extremely low fluorescence polarization (45). The disadvantage with this approach is the need for an additional fluorescence detector. Proof of principle is demonstrated is Fig. 4, which shows the response of both detectors as fluorescein was added to a culture of yeast cells expressing GFP. While the magnitude of the

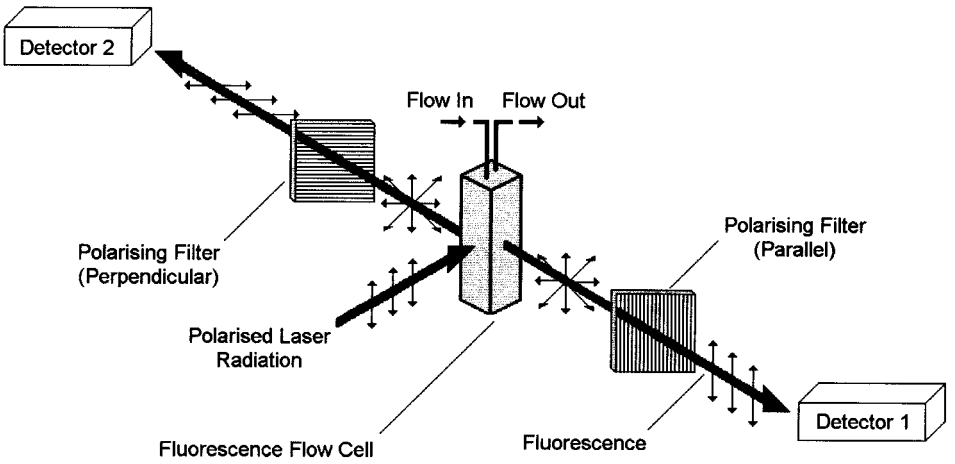

FIG. 3. Schematic diagram of the fluorescence polarization experiment incorporating a flowthrough optical cell.

fluorescence signal on each channel increased linearly with fluorescein concentration, the difference signal ($I_{||} - I_{\perp}$) due to the GFP present remained constant. Hence, the signal due to fluorescein, used to simulate autofluorescence, was effectively cancelled out.

Provided the interfering species produces fluorescence that is less polarized than GFP, i.e., has a lower polarization ratio, then by taking a difference measurement ($I_{||} - I_{\perp}$), a greater percentage of the autofluorescent signal will be removed from the final measurement than that of the signal due to GFP. Hence, an increase in signal-to-noise ratio will result. The beauty of this method is that because it relies on a property of the light other than wavelength, it can be used to discriminate GFP from autofluorescence with substantially the same spectral properties.

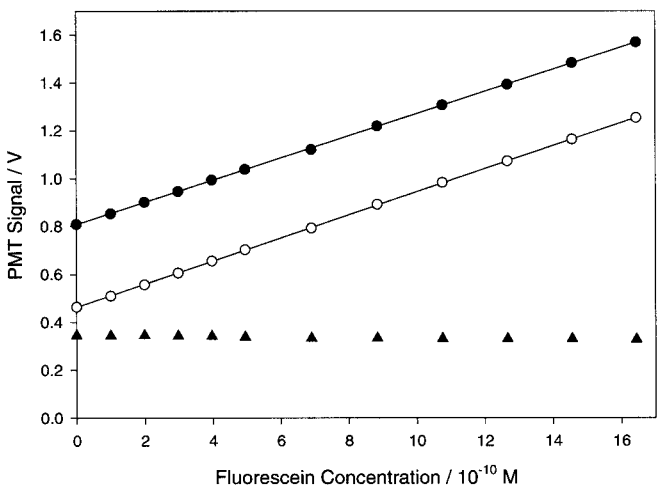

FIG. 4. Variation in fluorescence signals as fluorescein is added to a culture of genetically modified yeast cells expressing GFP. (●) Fluorescence signal from the parallel filter detector 1 ($I_{||}$). (○) Fluorescence signal from the perpendicular filter detector 2 ($I_{\perp}$). (▲) The signal for GFP, taken as the difference between these respective measurements ($I_{||} - I_{\perp}$). The lines shown are the linear regressions of the measured fluorescence signal versus fluorescein concentration. Reproduced from Ref. 45, with permission of the Royal Society of Chemistry.

Postmeasurement Image Correction (Use of Image Analysis Software)

Fluorescence microscope images captured using digital cameras, or CCD detectors can be manipulated using image analysis software to improve the discrimination of GFP-laden cells, or labeled cell components, over background autofluorescence. Most commonly available image manipulation software packages will allow simple adjustments of brightness, contrast, and sharpness, for example, that may improve any type of image. In addition, the feature of automatic edge detection may allow GFP-labeled cell structures to be specifically highlighted. With a color image, given sufficient wavelength separation between GFP and autofluorescence, adjustments such as color balance, hue, and color transformations may also be applied. For example, this may be useful where the pure green of GFP fluorescence is seen against yellow–green autofluorescence. The simplest and crudest method to select green fluorescence from a color image is to convert it to red–green–blue (RGB) format, and display only the green channel signal. All of these transformations are however somewhat subjective and involve corruption of the original data. Such transformations are usually carried out to enable qualitative observations or for aesthetic enhancements.

The authors have used a method of analyzing pixel brightness to remove autofluorescence contaminating fluorescence microscope images of GFP-laden yeast cells, which is demonstrated in Figs. 5 and 6. Some image analysis software packages, such as Corel Photo-Paint, are able to analyze the brightness of in-

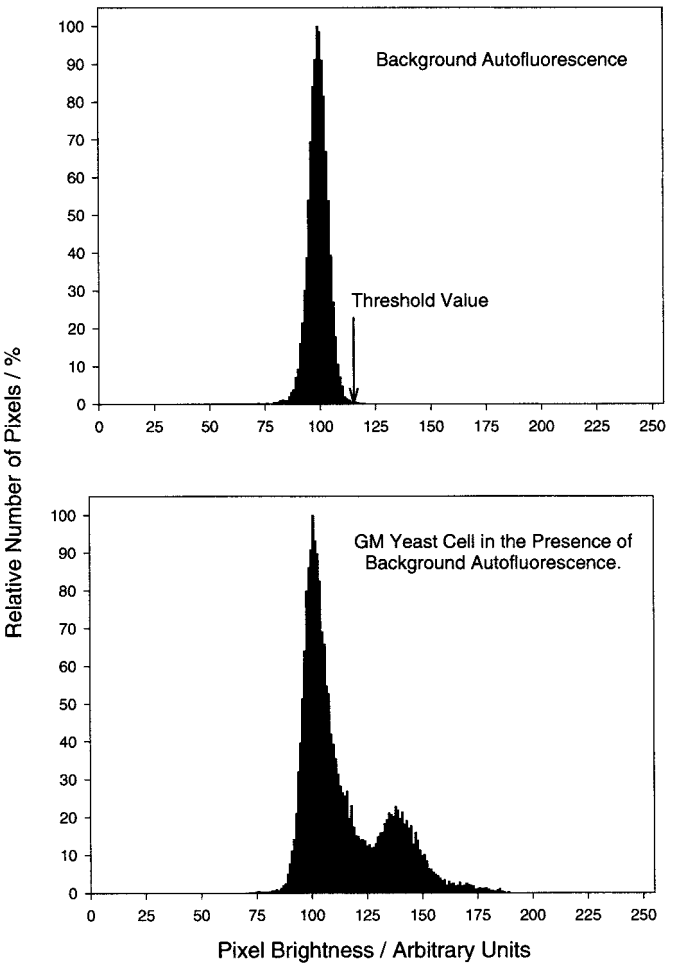

FIG. 5. Two intensity histograms showing pixel brightness distributions for images of background autofluorescence and a GM yeast cell in the presence of autofluorescence.

dividual pixels in an image. A histogram is produced showing the number of pixels of each brightness on a scale from 0 to 255, where 0 is black and 255 is pure white on a monochrome image, or pure bright green on the green channel of an RGB image. In our application, yeast cells were genetically engineered to express GFP in response to DNA damage repair (47). Fluorescence microscope images showed distinct background autofluorescence originating from the growth media, which to some extent obscured the yeast cells. It was found that analysis of pixel brightness in areas of the image containing only autofluorescence showed a particularly narrow distribution in brightness values. In other words, the intensity of the background autofluorescence was quite uniform across the microscope image. When an area of the image containing a yeast cell was analyzed, the same narrow pixel brightness distribution of the autofluorescence was still visible, but it was alongside a wider distribution of brighter pixels that comprised the image of the yeast cell. Using the analysis of the pure autofluorescence, a threshold value of brightness could be selected above which the autofluorescence was not visible. In the example shown in Fig. 5, this value was chosen as 115. The software can then remove from the image all pixels which fall below the threshold value, and thus the autofluorescence is stripped from the image leaving the yeast cells clearly visible, as shown in Fig. 6.

Furthermore some quantitative data can then be derived. The total GFP fluorescence intensity, proportional to GFP concentration, can be obtained by integrating pixel intensity above the threshold value by pixel count (48). However, if the source of the autofluorescence physically overlaps that of the GFP under the microscope, it will contribute toward the apparent GFP brightness and will need to be estimated and subtracted. Second, there may also be a need to calibrate the brightness measurement with the fluorophore concentration, rather than assume that a pixel brightness value of 100, for example, represents twice the concentration of GFP with a brightness of 50. This could be readily carried out with fluorescein. Third, the thickness of the sample beneath the microscope slide would need to be uniform and reproducible. Dual wavelength fluorescence correction techniques, if relevant, can also be applied to images since the same software will usually allow the subtraction of two images.

Confocal Laser Scanning Microscopy

Confocal laser scanning microscopy (CLSM) is an established technique for obtaining high-resolution fluorescence images and three-dimensional reconstructions of a variety of biological specimens. In CLSM, an expanded laser beam is reflected by a dichroic mirror and focused to a small spot within the sample by means of a microscope objective lens. The fluorescence produced is collected by the same objective and passes through the dichroic mirror toward a photomultiplier. A confocal aperture (a pinhole, typically a few hundred micrometers in diameter) is placed in front of the photodetector. This is positioned such that fluorescent light from points within the specimen that are outside the focal plane of the laser, "the out of focus light," is obscured from the detector. In this way it is possible to carry out "optical sectioning," as the laser is swept back and forth across the sample. The analogue light signal from the photomultiplier is converted to a digital signal and recorded as a function of laser position in a pixel-based image constructed by a computer. By building up a series of images it is possible to perform depth profiling and produce a three-dimensional image of the sample (49, 50).

However, if the autofluorescence occurs at a wavelength similar to that of GFP and if the autofluorescent species is evenly dispersed throughout the area of in-

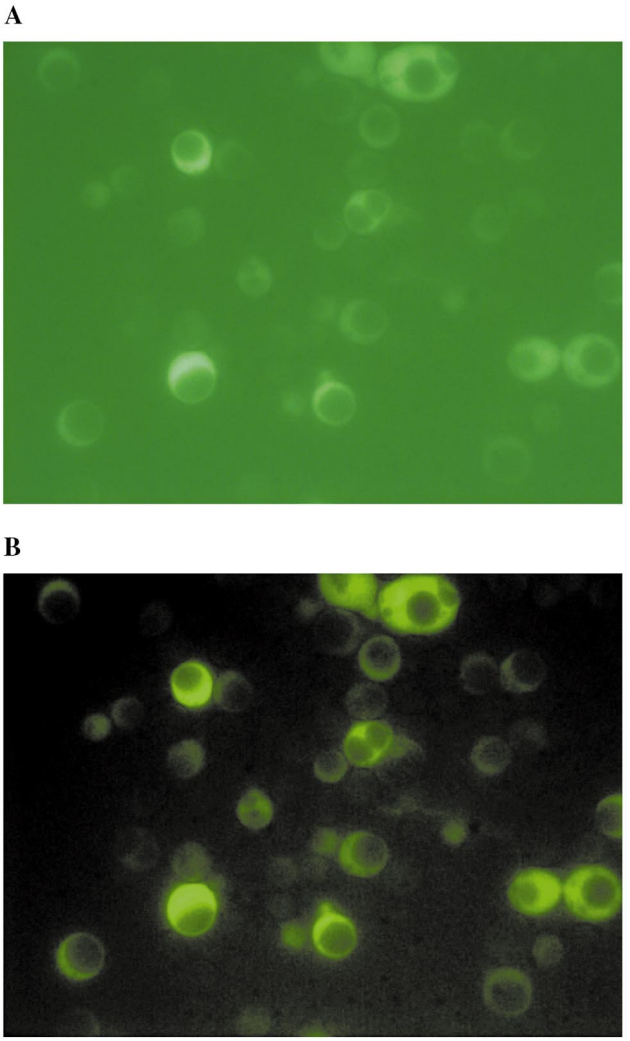

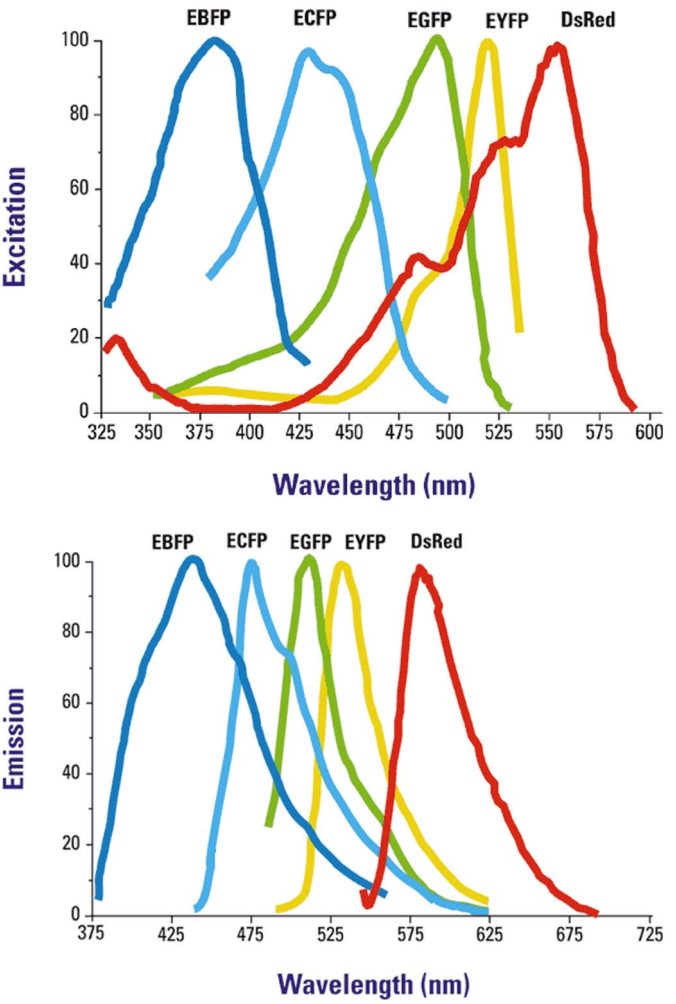

FIG. 6. (A) Fluorescence microscope image of yeast cells expressing GFP in medium showing autofluorescence. (B) The same fluorescence microscope image after software correction to remove autofluorescence (see text for details). Photograph courtesy of M. G. Barker and J. A. Miyan, Department of Biomolecular Sciences, UMIST.

FIG. 8. Excitation and emission spectra for enhanced blue, cyan, green, yellow, and the newly discovered DsRed fluorescent proteins, demonstrating the diversity of excitation and emission wavelengths currently commercially available in fluorescent proteins. Reproduced with permission from Clontech Laboratories, Inc. (Palo Alto, CA).

terest within the sample, then CLSM is susceptible to the same problems with autofluorescence as other conventional microscopy techniques. The main advantage of CLSM stems from restricting the excitation light to that material confined within the confocal spot, in cases where either the GFP or autofluorescence is highly localized. Thus, discrete subcellular compartments can by specifically analyzed, either by picking out just the areas of the sample where GFP has been targeted or by avoiding areas where autofluorescence is more prevalent. The focused laser could also be used to photobleach specific autofluorescent areas of the sample. The main drawback of this technique is the inefficient use of excitation light. Only fluorescence photons which pass back unhindered through the sample matrix to the detector will be detected. Scattered photons, which are often in the majority, are excluded by the confocal aperture. The increase in the intensity of the excitation light needed to compensate for this loss results in increased photobleaching of the sample, both at the focal spot and along the light path passing through the sample matrix.

Two-Photon Laser Scanning Microscopy

The main disadvantage of CLSM, discussed above, can be largely avoided by the use of two-photon laser scanning microscopy (TPLSM). In TPLSM, short pulses of near-infrared laser light (typically 100 fs at 100 MHz) are focused onto the sample in the same way,

and using essentially the same instrumentation, as for CLSM. Two-photon excitation occurs upon simultaneous absorption of two separate photons, each having half the energy required to cause transition to the excited state. For example, 778-nm light is used to produce excitation at 389 nm, which has been used to image GFP in mammalian cells (49). The very steep dependence of the absorption rate on light intensity in TPLSM means that excitation and subsequent fluorescence only occur within the diffraction limited focal spot, where light intensity is high. Virtually no fluorescence excitation occurs above or below the focal spot; hence, a confocal pinhole is not required for spatial resolution. Most fluorescence photons, whether scattered on leaving the sample or not, can be collected and contribute toward the measured signal. Thus the sensitivity of the technique is enhanced and lower intensity excitation light can be employed which in turn reduces photobleaching (51). Scattered and reflected excitation light is easily removed from the fluorescence emission due to the large wavelength separation. The longer wavelength also penetrates sample tissue more readily. In addition, any scattered excitation light will be too weak to promote two-photon excitation of other fluorescent material outside the area of interest.

This approach does however have some disadvantages. The first is the need for a more complex and expensive pulsed laser light source. The second is that common wavelengths from infrared lasers produce excitation at wavelengths significantly lower than the optimum 490 nm. At such wavelengths, autofluorescence can increase due to more efficient excitation of NADH, and photobleaching of GFP has been reported to be more rapid (49).

Time-Resolved Fluorescence Microscopy

Time-resolved fluorescence spectroscopy is often used to quantify fluorescently labeled species in the presence of nonspecific background autofluorescence. In its simplest form a pulsed light source is used, and the fluorescence of the labeled species is measured after a time interval in which the short-lived autofluorescence has decayed. The method is best applied to fluorescent species with especially long fluorescent lifetimes (>15 ns), such as some transition metal or lanthanide chelates. Since GFP has a particularly short fluorescent lifetime (2.6 ns for S65T GFP), this approach may be less suitable; however, its success will depend on the fluorescence lifetime characteristics of the autofluorescence specific to a given application.

The fluorescence lifetime of different GFP mutants varies considerably, from 1.3 ns for cyan fluorescent protein to 3.7 ns for yellow fluorescent protein. This variation has enabled different GFPs to be distinguished in multiple labeling applications using time resolved techniques. Pepperkok *et al.* (52) used fluorescence lifetime imaging microscopy (FLIM) to resolve three coexpressed GFP mutants. In FLIM, the excitation light source is a pulsed laser and images are captured using conventional optics with a time-gated CCD or similar detector. A series of time-gated images are collected between each excitation pulse, and therefore the decay of fluorescence is recorded simultaneously for each pixel in the field of view. Software algorithms combine the data from each successive image to determine the fluorescence lifetime for each pixel. Data collection and subsequent processing typically take a few minutes to complete and result in a series of fluorescent lifetime maps, each highlighting a different range of fluorescent lifetimes and thus different species. Provided the average fluorescence lifetime of the GFP mutant used and the autofluorescent species are significantly different, this approach should enable the two to be distinguished. Since the parameter measured is a spectroscopic property other than wavelength, only a single dichroic and long-pass filter is required. This enables a large proportion of the light emitted to be recorded, enhancing sensitivity, and thus lowering the intensity of the excitation light needed. This in turn reduces photochemical degradation of GFP. The resolving power of the technique can also be increased by combining the fluorescence lifetime and wavelength information.

The main disadvantage of this technique is the need for complex and expensive instrumentation, including a pulsed laser and fast image acquisition and data processing hardware. In addition, the fluorescence lifetime of GFP mutants is affected by temperature, fusion to other proteins, and to a lesser extent variations in pH. For example, Pepperkok *et al.* observed a 400-ps decrease between room temperature (22°C) and 37°C, and a 400- to 500-ps decrease upon fusion to another protein.

Capillary Electrophoresis

Capillary electrophoresis (CE) is a powerful electroseparation technique, which is widely used in biochemical analysis due to the small sample volumes required, rapid analysis time, high resolving power, and the ability to directly inject samples. Molecules to be separated migrate through a buffer solution under the influence of an electric field, with mobilities that depend on their molecular size and charge. Separation takes place in a capillary tube, across which a voltage of typically tens of kilovolts is applied. Capillary electrophoresis has been used as a method to physically separate GFP from other autofluorescent species in media and cellular extracts, and to allow its direct quantification. Using CE, GFP is best detected using laser-induced fluorescence. Fluorescence is collected at

90° to the capillary using a microscope objective, coupled with a spatial mask and photomultiplier tube. Low limits of detection for both wild-type (53) and S65T GFP (54) have been reported, which are in the order of 10^{-12} M. With the low injection volume of CE, typically around 20 nl, this limit of detection corresponds to approximately 10^{-20} mol, or just a few thousand molecules.

For CE, cellular extracts containing GFP must be carefully prepared by laborious procedures including repeated washing and lysis of the cells, followed by centrifugation, filtration, and resuspension steps. However, once prepared, GFP can easily be separated from other autofluorescent species and quantified. For example, Fig. 7A is an electropherogram showing the separation of S65T GFP from autofluorescent media impurities, in the analysis of an extract of human embryonic kidney (HEK293) cells, from the work of Malek and Khaledi (54). These workers have also reported the quantification of GFP in whole HEK293 cells using CE, without the need for cell lysis, as shown in Fig. 7B. In this way, cells can be effectively separated from autofluorescent media components and then GFP can be quantified on a cell by cell basis. The resolving power of CE will also allow separation of different forms or mutants of GFP, even if their wavelength characteristics are identical, since separation depends on structural properties. For example, Korf *et al.* separated the two naturally occurring isoforms of wild-type GFP in under 5 min using a simple borate buffer at pH 8.5 (55). Similarly, free and immune-complexed GFP can be resolved.

One disadvantage of the technique is the need to optimize the buffer conditions, such as ionic strength and pH, to suit both the electroseparation and the GFP fluorescence, and in the analysis of whole cells, also maintain the cell integrity. Interestingly, adverse conditions that severely impair the fluorescence of free GFP have been found not to diminish fluorescence detection of immune-complexed GFP (55). However, CE is inherently a disruptive and invasive technique, in terms of either the need for cell lysis, or in removing cells from growth media for analysis in a separation buffer, and it requires expensive instrumentation including a high voltage power supply and components for laser-induced fluorescence detection.

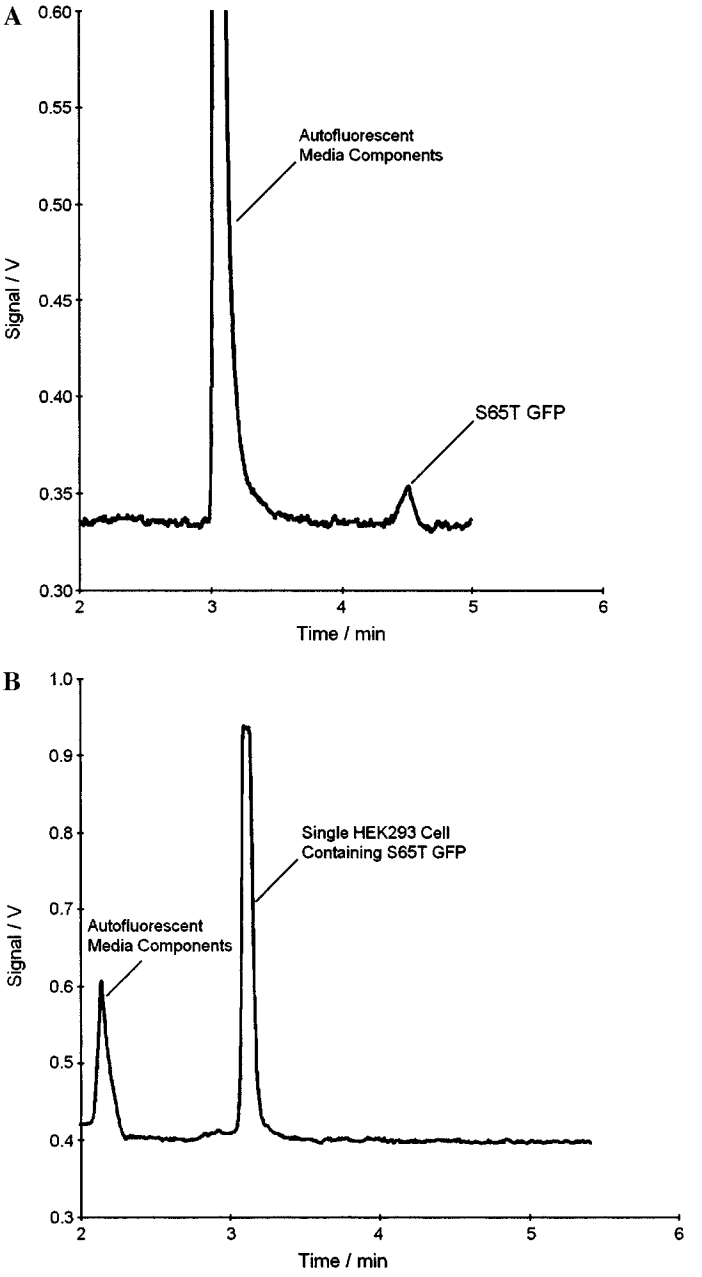

FIG. 7. Electropherograms of (A) the separation of S65T GFP from autofluorescent components in HEK293 cell extract. Buffer: 10 mM Tris–HCl, pH 7.5. Applied voltage, 40 kV. (B) The separation of a single HEK293 cell containing GFP from autofluorescent media components. Buffer: 10 mM Tris–HCl, pH 8.0. Applied voltage 40 kV. Adapted from Ref. 54.

CHEMICAL/PHOTOCHEMICAL METHODS OF REDUCING AUTOFLUORESCENCE

Choice of Growth Medium

Careful choice of growth medium might seem to be an obvious and simple way of reducing autofluorescence, but it can be crucial in enabling the detection of *in vivo* fluorescence. This was particularly relevant in the early stages of our own work requiring detection of fluorescence from GFP, expressed in *Saccharomyces cerevisiae* (56). The combination of a weak promoter (from the *RAD54* gene) driving expression of an S65T derivative of GFP and an intensely autofluorescent growth medium, made *in situ* GFP detection extremely difficult.

The first step in improving the fluorescence detection system was to remove as much contaminating medium fluorescence as possible. To achieve good yields of cells, a complex rich medium (YPD, yeast extract, peptone, and dextrose) (57) was initially used. However, this particular medium emits intense broad band fluorescence centered at 511 nm, the wavelength used to detect S65T GFP fluorescence. The combination of poor expression and weak emission meant that the GFP signal was completely masked by autofluorescence in this medium.

A complex minimal medium (SD, synthetic dextrose medium) (57) was utilized as a lower fluorescent alternative. SD was found to produce 10-fold less autofluorescence at the GFP emission wavelength than the rich counterpart, but still resulted in a poor signal-to-noise ratio. A defined minimal medium, normally employed in fermentation experiments [adapted from (58)], was subsequently tried. This medium does not contain the highly fluorescent component of SD, yeast nitrogen base. The investigator has complete control over the constituents of the fermentation medium (called F1), allowing it to be refined to specific requirements. The basic composition of F1 is a mixture of inorganic salts, trace elements, and vitamins, supplemented with glucose and additional nutrients according to auxotrophic requirement. Thus, the levels of autofluorescent components can be minimized, resulting in negligible autofluorescence (600-fold less than the rich medium).

Medium fluorescence is a common problem, often mentioned in passing under Materials and Methods sections of publications. For example, one group attempting to use GFP as a quantitative reporter of promoter activity in *E. coli* note that LB (Luria-Bertani) broth is unsuitable for the liquid culture of GFP-expressing cells due to its "high and variable background fluorescence" (59). One of the constituents of LB is intensely fluorescent yeast extract. The problem was overcome by employing M9 minimal medium, a defined mixture of salts supplemented with the appropriate carbon source and amino acids if required. A further method for overcoming this problem is to change the medium prior to fluorescence measurement. Phosphate-buffered saline can be used as a predetection washing agent to remove contaminating fluorescent species and it also behaves as a low background fluorescence detection medium (10, 60). However, it is noteworthy that removal of autofluorescent growth medium from cells by washing can reduce the longevity of fragile cells on the microscope slide. Hence, observations must be made rapidly before cell lysis occurs.

A more involved method was utilized by Aubin (11). Various mammalian cell lines were grown in specific media, supplemented with calf serum. Aubin extracted fluorescent components from the serum using dextran–charcoal treatment. After mixing and incubating at room temperature, the charcoal was removed by centrifugation and the serum was further purified by microfiltration. This process removed 95% of detectable fluorescent components.

Finally, many growth media contain phenol red as a pH indicator to ensure that the growth medium is not contaminated. This indicator can interfere with GFP fluorescence detection and therefore the use of a phenol red-free medium is suggested.

Selection of low autofluorescent culture medium from the outset or prior to fluorescence detection may not always be practicable, but where possible, it is certainly one of the simplest approaches for the reduction of background autofluorescence.

Chemical Treatment

The abrogation of media autofluorescence can still leave significant disruptive fluorescence from intracellular sources or residual species after extraction. Aside from the instrumentation methods discussed, there are specific chemical treatments that can be employed to aid autofluorescence discrimination.

Of particular importance, given their culpability in cellular autofluorescence, is the redox state of pyridine dinucleotides and flavins. The pyridine dinucleotides are primarily fluorescent in the reduced state (NAD(P)H) while the flavins are more fluorescent in the oxidized state. Flavins can be chemically reduced to lessen their fluorescent contribution. Metcalf reduced riboflavin by injection of a weak solution of sodium dithionite, but also noted that the nonfluorescent state was transient, fluorescence returning slowly with reoxidization by air or rapidly with dilute hydrogen peroxide (9). Dithionite reduction is still used as an assay for the presence and concentration of flavins by measuring the change in fluorescence emission at ~520 nm before and after reduction (61, 62). However, the application of this method to the reduction of autofluorescence must come with the caveat of unknown consequences for pyridine dinucleotide fluorescence. As Schneckenburger *et al.* point out (14), altering the redox state of one of these two coenzymes will concomitantly enhance the autofluorescence of the other. Another way of reducing oxidized flavins lies in their light sensitivity. Irradiation with light in the presence of electron donors such as EDTA readily reduces oxidized flavins (63). Further treatments for the inhibition of flavin fluorescence include cyanide and hypoxia (59), although cyanide also reduces the nicotinamide nucleotides to the fluorescent state (13). Bessey and co-workers (64) showed that FAD fluorescence could be quenched by the presence of purines such as, adenosine, adenine, and adenylic acid.

Lipofuscin is thought to accumulate mainly in postmitotic cells, so utilization of such cells for fluorescence studies should be avoided where possible. Schnell *et al.* (20) studied the effect of chemical treatments on tissue sections from monkey, rat, and human neural tissue. They revealed that lipofuscin-like autofluorescence in these tissues could be significantly reduced or eliminated by treatment with 1–10 mM $CuSO_4$ in a 50 mM ammonium acetate buffer (pH 5) or 1% Sudan black B in 70% ethanol. The same group investigated the effects of these treatments on immunofluorescent labeling and found that pretreatment with $CuSO_4$ or Sudan black B also reduced the intensity of the immunocytochemical labeling (20). While $CuSO_4$ reduced immunofluorescence in a dose-dependent manner, its effects on lipofuscin-like autofluorescence were more pronounced.

Choice of Fixative

An attractive property of GFP for microscopists is its tolerance to fixatives such as formaldehyde and glutaraldehyde (65). Retention of GFP fluorescence in such fixatives allows viewing and localization of GFP in preserved tissue. However, formaldehyde enhances autofluorescence from flavins (60) in all cell types and glutaraldehyde has a tendency to yellow with age and develops a bluish fluorescence which may interfere with the GFP signal (66). The use of formaldehyde as a fixative can diminish the fluorescence of some GFP fusion proteins (67) while others precipitate out of solution, forming misleading bright spots throughout the cell (68). The use of either of these fixatives prior to viewing GFP fluorescence means that the cells or tissue should be thoroughly washed to remove all traces of the chemical. GFP is very sensitive to some nail polishes used to seal coverslips onto microscope slides (65) and so the use of molten agarose or rubber cement is recommended as a sealant. Complete loss of GFP fluorescence is observed in the presence of absolute ethanol (66), making it unsuitable as a fixative and also implying that GFP fluorescence is unlikely to withstand the complete dehydration required for paraffin or plastic embedding. Mounting and embedding media, also used for sectioning work, can be an additional source of autofluorescence. Those of natural origin, such as Canada balsam or glycerin–albumin are among the worst culprits, and hence the use of one of many commercially available, synthetic, low fluorescence mounting media is recommended. Note that water-soluble resins are preferable if the mount is to be removed before viewing with a fluorescence microscope, as the use of alcohol will diminish GFP fluorescence.

Selection of pH

In studies on rat liver cell membranes (62), it was shown that while dithionite reduces flavins to a very low fluorescent state, treatment with hydrogen peroxide to reoxidize the flavins did not restore 100% fluorescence. Dithionite reacts with hydrogen peroxide to produce sulfuric acid, thus lowering the pH. It was the change in pH that was responsible for preventing full restoration of flavin fluorescence (64, 69). Hence, flavin fluorescence can be pH controlled. This is further corroborated by research into eosinophil autofluorescence, in which FAD fluorescence is quantified by the difference between the fluorescence intensity at pH 7.7 and 2.6 (70).

However, care should be taken in adjusting the pH to control autofluorescence, as the intensity of GFP fluorescence is also pH-dependent. While the wild-type GFP shows a relatively constant brightness from pH 5 to 10, the commonly used S65T mutants are twofold brighter at pH 7 than at pH 6 (71).

Purification

If GFP localization or fluorescence at the individual cell level is not a requirement, it is possible to extract GFP for fluorescence quantitation. The high stability and fluorescence durability of GFP make it suitable for extraction. GFP fluorescence is only eliminated by harsh conditions including extreme pHs, 6 M guanidinium chloride at 90°C, or 1% SDS at 65°C (72).

A crude extraction previously employed in this laboratory was adapted from the method used by Johnson and Kolodner (73) and is detailed elsewhere (56). Yeast cells expressing GFP were repeatedly washed in water followed by an "extraction" buffer to remove all traces of medium fluorescence before resuspension in a "crushing" buffer. Cell lysis was performed by vortexing with 0.45-μm diameter glass beads and cell debris was removed by centrifugation after removal of lysate from the beads. The resulting crude extracts were adjusted to pH 11 with 1 M TRIS-base and then assayed for GFP fluorescence. After measurement, extracts were treated with 1% SDS at 65°C for 15 min to eliminate GFP fluorescence. Subsequent fluorescence measurement then allowed quantitation of the proportion of autofluorescence in the GFP signal. This crude extraction procedure permitted detection of GFP fluorescence in cells that was otherwise inhibited by autofluorescence and absorption effects of the cellular matrix and cell wall.

Traditional protein purification techniques can be used to extract GFP after *in vivo* expression. Deschamps *et al.* employed chromatographic techniques to purify recombinant GFP from an *E. coli* expression system (74). After creating extracts from *E. coli*, ammonium sulfate at 40% saturation was added, leaving

GFP in the supernatant, and then increased to 70% saturation to precipitate GFP. The GFP was solubilized in ammonium sulfate for purification on a size-exclusion column, with elution by reduction of the salt concentration. The GFP concentrate was then passed through an ion-exchange column and GFP fractions were identified by spectroscopic characteristics. Further traces of contaminants were removed by a final HPLC size-exclusion step in low-salt buffer.

Purification of polyhistidine-tagged GFP has been demonstrated using a new purification matrix of ceramic hydroxyapatite ($Ca_5(PO_4)_3OH$) loaded with different metal ions (75). Zn(II) was found to be the best metal ion for this purpose. The tagged GFP bound to the column was eluted using either phosphate buffers or EDTA, that competed for phosphate groups in the hydroxyapatite or complexed with the metal ions. Buffered extraction procedures involving repeated centrifugation were still required to prepare GFP-containing cytoplasmic extracts.

A recent paper demonstrated that organic solvent purification of GFP from *E. coli* is possible (76). The soluble protein fraction was collected after sonication of cells, followed by removal of nonfluorescent, insoluble material. Ammonium sulfate was added to the green fluorescent supernatant to a final saturation level of 70% before ethanol extraction. GFP was then extracted back into an aqueous phase from the ethanol extract, using less polar solvents. The GFP content of this extract was found to be more than 90% of the total proteins with a yield of ~60% of the total GFP present initially. The final step in the purification was phenyl-Sepharose chromatography and the resulting GFP showed the appropriate spectroscopic characteristics.

Numerous fusions of cellular proteins or signal peptides with GFP have been made to follow real-time protein translocations (77–81) and kinetics of protein secretion (82–84). Secretion of GFP from cells into the surrounding media could be used to enhance its detection since cellular autofluorescence and scattering problems are removed. Laukkanen *et al.* (85) demonstrated that GFP could be secreted from insect cells into the culture medium, giving easily detectable fluorescence. Combined with the utilization of low autofluorescence culture medium or phosphate-buffered saline, this could be a sensitive method of GFP quantitation.

Autofluorescence Quenching

Fluorescence quenching is a simple *in situ* method of reducing nonspecific autofluorescence without the need for additional instrumentation or optics. Microscope sections or whole cells for cytometry are stained with an appropriate dye which, for example, quenches the broad band autofluorescence, while allowing visualization of the narrower band GFP fluorescence. For effective quenching the dye used should have an absorbance spectrum that significantly overlaps that of the autofluorescence emission. For example, van der Geest and Petolino stained transgenic plant tissue sections with toluidine blue to allow the detection of wild-type GFP, which was otherwise obscured by cellular autofluorescence (7). Sections were stained for 30 s in 0.5% toluidine blue, which significantly quenched cell wall autofluorescence. Nontransformed, control sections stained with the dye showed no appreciable fluorescence. Toluidine blue has a peak absorbance at 626 nm, while absorbance at 400 and 500 nm is low, at only 2 and 12% of the peak respectively. Other dyes which have been successfully used for quenching autofluorescence include methylene blue (peak absorbance 668/609 nm) and trypan blue (peak absorbance 607 nm) (86). Fluorescence emission from these compounds occurs in the far red region of the spectrum and is thus easily blocked with appropriate filters.

Provided a dye with suitable spectroscopic properties for a given application is available, there are several further criteria to fulfill. The dye chosen should be able to permeate cell membranes, otherwise a cell permeabilization process is required. A low-molecular-weight facilitates this and also ensures rapid diffusion throughout the cell. However, since autofluorescence is often concentrated in particular structures or regions of the cell, the dye also needs to be able to evenly diffuse into these specific intracellular areas. The dye should also exhibit low cytotoxicity if it is to be used in real time *in vivo* studies. Finally the concentration of the dye used must be carefully optimized, as too high a concentration will significantly quench the GFP fluorophore. Finding a dye to satisfy all these criteria is the main disadvantage of this technique.

Drosophila

In preparing live eggs for imaging, the highly autofluorescent chorion can be easily removed by pulling on the dorsal appendages of oocytes with fine-tipped forceps or by rolling the embryos gently on a piece of double-sided sticky tape (87). Since the autofluorescence of *Drosophila* is very much localized to specific structures, confocal microscopy is particularly applicable (see earlier section).

Photochemical Methods (Photobleaching, Photoconversion, and FRET)

Several workers have observed that when viewing GFP-labeled cells or organelles under the microscope, the broad spectrum yellow–green autofluorescence of the surrounding media or cellular material tends to fade with prolonged illumination, and the GFP signal

is then more readily resolved. This is presumably due to photobleaching of the autofluorescent species.

GFP is relatively resistant to photobleaching, its photochemical stability arising from the fact that the fluorophore element of the protein is encapsulated within the barrel-like structure, well shielded from chemical reactants such as O_2. The rate of photobleaching of wild-type and S65T GFPs is reported to be less than half that of fluorescein (46, 88). This difference in photobleaching rates between GFP and other fluorescent species may be exploited to enhance the detection of GFP in the presence of autofluorescence. Improvements may be observed when using a fluorescence microscope, for example, if the image is captured several seconds after the sample illumination has been switched on. However, care should be taken if this approach is to be adopted for quantitative work, since GFP will also be photobleached to some extent during this period, and the rate of photobleaching may vary depending on the presence of modulating species in the surrounding medium. The use of antifade agents such as Vectashield (Vector Laboratories, Inc., Burlingame, CA) as mounting media for fluorescence microscopy can reduce the rate of photobleaching and hence increase the measurement and integration time available for imaging. This can result in clearer images and improved GFP signal discrimination.

Zylka and Schnapp have used a photobleaching method to reduce interference from media autofluorescence, thought to originate primarily from riboflavin, when imaging live mammalian cells (39). In order not to unduly illuminate the cells expressing GFP, a small volume of growth medium alone was exposed to short-wavelength UV light for 2 min, in a light box containing four 15-W, 300-nm bulbs. Shortly before viewing the cells, their growth medium was replaced by the UV-treated medium. In addition to photobleaching autofluorescent compounds, this method may, however, destroy media components which are critical for sustaining the cells, or form photochemical derivatives harmful to the cell. The process of switching media prior to measurement also necessitates an extra laborious step and thus may be less suitable for realistic real-time monitoring of GFP *in situ*.

Any method that enables excitation of a particular GFP to occur at an alternative wavelength may be useful in avoiding areas of the spectrum which preferentially excite autofluorescent species. Similarly methods which enable the fluorescence emission of GFP to be shifted to an alternative wavelength may help to avoid areas of the spectrum where autofluorescence is primarily occurring. A few such methods exist, however they have yet to be applied specifically to improving autofluorescence discrimination.

Wild-type GFP shows a major absorption/excitation peak at 395 nm with a lesser peak at 475 nm, and emission centered at 508 nm. It has been known for some time that prolonged irradiation of wild-type GFP with UV or blue light causes a progressive decrease in the 395 absorption peak, and corresponding increase in the 475-nm absorption peak, due to photo-induced isomerism of the molecule (88, 89). This occurs especially with UV irradiation in the range 280–395 nm, but is also observed with blue light up to 490 nm (71). The photoconversion process reverses only slowly over a period of days in the dark (89). Thus, by first irradiating wild-type GFP with UV light, the major absorption peak can be effectively moved from the UV to the blue region of the spectrum. The use of 475 nm for excitation thus reduces autofluorescence from species such as NAD(P)H which primarily absorb in the UV. However, during illumination, photobleaching processes will also occur causing both 395 and 475 nm absorption peaks to decline by approximately the same extent, with a corresponding loss in sensitivity. Blue excitation-enhanced GFPs, such as S65T and its derivatives, do not show the UV absorption peak or this form of photoisomerism, only slow photobleaching upon illumination with UV or blue light (88).

Elowitz *et al.* discovered that a variety of GFPs, including wild-type, S65T, and EGFP, can undergo a photoconversion to a red fluorescent species upon irradiation with blue light, from an argon-ion laser or microscope lamp, under anaerobic conditions (90). The red fluorescent species thus formed absorbs green light at 525 nm and fluoresces with a maximum at 600 nm. Thus GFP photoactivated in this way can be viewed using a rhodamine filter set. Anaerobic conditions can be brought about by the use of oxygen scavengers such as a combination of glucose oxidase, catalase, and glucose, or occur in microorganisms housed in a sealed environment that have exhausted their available oxygen. This low oxygen concentration requirement is in contrast to the need for oxygen in the latter stages of chromophore development after GFP expression. The red-emitting form of GFP remains stable for at least 24 h, but its chemical nature is currently unknown. After exposure to a flash of blue light the red emission develops relatively slowly with a time constant of 0.7 s, suggesting that photoactivation is a two-stage process: irradiation stimulating fast transition to an excited intermediate, which subsequently decays slowly to the red emitting state, the latter process occurring even the dark. Thus by photoactivation in this way both the excitation and emission characteristics of GFP can be radically altered.

Fluorescence resonance energy transfer (FRET) is a phenomenon whereby a fluorescent molecule, the donor, transfers excitation energy in a nonradiative way, usually by dipole–dipole interaction, to a neighboring fluorophore, the acceptor. Energy transfer requires that the emission spectrum of the donor fluorophore,

overlaps that of the absorption spectrum of the acceptor fluorophore, and that the two fluorophores are in very close proximity (<100 Å apart) with their respective transition moments at an angle other than 90° to each other. Chromophore-mutated GFPs show excellent spectral overlap and hence make good FRET pairs (91). For example, BFP emits at 466 nm making it a good donor to enhanced GFP (S65T), which absorbs at 488 nm (92). A superior example is the pairing of cyan fluorescent protein (CFP), with emission at 505 nm, which is an excellent donor to the yellow fluorescent protein (YFP), with absorbance at 514 nm (91).

The efficiency of the FRET process is highly dependent on the proximity of the fluorophores, being inversely related with the sixth power of separation distance. Therefore it has mainly found applications in the study of protein–protein interactions, protein conformation changes, and proteolytic processes. However, FRET could be used to provide an alternative emission or excitation wavelength for a particular GFP mutant. The technique would require an additional GFP, i.e., the corresponding FRET partner. Their close spatial proximity can be achieved either by the expression of a fusion protein, with the two GFP mutants tethered by a short spacer of <20 residues (93), or by expressing the two GFP mutants separately, each with an appropriate protein tag attached that will subsequently strongly interact and thus bring the two GFPs together (92). The excitation and emission wavelengths of the GFP fusion protein are thus separated to a much greater extent than in the single GFP, and are 382 and 509 nm, respectively, for the BFP–EGFP pair, and 452 and 527 nm, respectively for the CFP–YFP pair. This makes the selection and optimization of optical filters easier and greatly reduces cross-talk interference, i.e., excitation light detected by the fluorescence detector. The disadvantages are obviously the need for greater genetic modification to allow expression of the additional GFP mutant, and that any biochemical effect that changes the distance between fluorophores or the relative orientation of their transition dipoles will significantly change the efficiency of the FRET process.

MOLECULAR BIOLOGICAL APPROACHES TO THE ENHANCEMENT OF GFP DETECTION

The Use of Spectrally Different GFP Mutants

The cloning of the wild-type GFP-encoding gene (94) from *Aequorea victoria* provided the means for creating new variant fluorescent proteins with altered fluorescence properties. In 1994, Chalfie *et al.* (65) showed that GFP was a genetically encoded reporter with no requirement for an enzymatic substrate or cofactor and, as such, could be expressed in both prokaryotic and eukaryotic cells, thus realizing its potential as a marker and reporter. Wild-type *Aequorea* GFP was originally used as the reporter molecule; however, its excitation at 395 nm results in increased background autofluorescence and photoisomerization, both properties that are undesirable in a reporter molecule. Thus, knowledge of the primary structure of GFP was used to create mutants with improved characteristics.

TABLE 3

A Selection of GFP Derivatives and Alternative Fluorescent Proteins with Diverse Spectral Characteristics throughout the Visible Spectrum

Fluorescent protein	Emission wavelength (nm)	Excitation wavelength (nm)	Reference
BFP/EBFP	440	380	(95)
CFP/ECFP	480	458	(95)
Wild-type GFP	508	395 (475)	(118)
EGFP	508	489	(101)
GFPuv	509	395	(119)
S65T GFP	510	488	(97)
yEGFP	515	490	(105)
YFP/EYFP	527	513	(96, 104)
DsRed	583	558	(28)

Table 3 lists some of the more common commercially available derivatives of GFP with the most pronounced spectral alterations. Several specific examples of mutations will be discussed below but others are discussed in detail elsewhere (see references in Table 3). Mutations in the 20 amino acids around and including the chromophore (residues 55–74) tend to alter the spectral characteristics and stability of the chromophore, while other mutations tend to affect protein folding and solubility. Table 3 and Fig. 8 illustrate the wide spectral diversity available from GFP mutants. This diversity allows the investigator to choose the most appropriate fluorescent protein with excitation and emission wavelengths significantly removed from those of the interfering autofluorescence.

Early GFP mutants with altered spectral properties were isolated by screening bacterial colonies after performing random mutagenesis. Heim *et al.* (95) isolated several mutants with altered spectral characteristics, of which two of particular interest are discussed here. One mutant was found to have a tyrosine to histidine substitution at position 66 (Y66H) that resulted in a significantly blue-shifted GFP derivative (BFP). This mutant was maximally excited at 382 nm with peak emission at 448 nm, although its fluorescence intensity was only 57%, relative to the wild-type GFP. The second mutant of interest was found to have a tyrosine to tryptophan substitution at position 66 (Y66W), resulting in another blue-shifted derivative, although not as significantly shifted as the BFP. The Y66W mutant exhibited maximal excitation at 458 nm and emission at 480 nm and is known as a CFP. Ormo *et al.* (96) used a site-directed approach to mutate threonine 203

(T203) which lies adjacent to the chromophore in the mature protein. A T203 to tyrosine (T203Y) mutant, which also incorporated two other chromophore mutations, had excitation and emission peaks of 513 and 527 nm, respectively. These red-shifted spectral characteristics were significantly different from other mutants and were distinguishable using the appropriate filter sets on a fluorescence microscope. This new mutant was termed a YFP.

Use of Specifically Enhanced GFPs

A key way of increasing the GFP fluorescence to autofluorescence ratio is to increase the fluorescence intensity of the GFP chromophore itself. Thus, the mutation approach has also been applied to enhancing GFP fluorescence intensity. The first breakthrough in fluorescence intensity-enhancing mutations was made by Heim *et al.* (97) after employing site-directed mutagenesis to create a point mutation at position 65, within the chromophore. Four mutants were obtained and all four showed a single excitation peak between 470 and 490 nm, with the loss of the unstable 395-nm excitation peak. The mutant with a serine to threonine substitution at position 65 (S65T) was selected since it exhibited the longest wavelengths of excitation and emission (489 and 511 nm, respectively), which more closely matched the standard fluorescein filter sets. Formation of the mature fluorophore also occurred 4-fold faster in the S65T mutant than in the wild-type protein. The peak amplitude of excitation for S65T was ~6-fold greater than for the wild-type and the emission peak amplitude was up to 8-fold greater.

A further study (98) on the effects of randomly mutagenizing the 20 residues around the chromophore also created serine 65 (S65) mutations. However, mutants selected by fluorescence intensity (10- to 110-fold more intense than wild-type) were found to have at least one mutation in addition to an S65 to alanine, glycine, or threonine substitution. The dual and triple mutants were found to have improved solubility when expressed in bacteria, in addition to the shift in maximal absorbance to between 480 and 501 nm. After accounting for the increase in protein solubility, the fluorescence per unit of soluble protein was shown to be 19- to 35-fold greater than for the wild-type protein. Increases in fluorescence intensity of this order have since greatly improved the sensitivity of GFP assays, especially in the presence of autofluorescence.

Codon Optimization and the Use of More Active Promoters

While GFP can be expressed in a large number of different organisms, the levels of expression vary widely between organisms. Low expression is a problem particularly in higher eukaryotes resulting in low signal-to-noise ratios in the presence of background autofluorescence. A synthetic *GFP* gene, EGFP (enhanced GFP), was created that incorporated 190 silent base mutations, giving an open-reading frame composed entirely of preferred human codons (99, 100). EGFP has been shown to exhibit 17-fold brighter fluorescence than the S65T derivative in human embryonic kidney cells (101). Human codon-optimized versions of blue, cyan, and yellow fluorescent proteins (EBFP, ECFP, and EYFP, respectively) have also been developed (96, 102, 103, 104) (see Fig. 8 for excitation and emission spectra for the enhanced fluorescent proteins and DsRed).

The technique of species-specific codon optimization has been transferred to a fungal version of GFP. Cormack *et al.* (105), developed a yeast-enhanced GFP (yEGFP) by optimizing the codon usage in the *GFP* gene for *Candida albicans,* which uses a noncanonical genetic code. Two amino acid substitutions that were previously shown to increase fluorescence intensity (97) were also incorporated. In contrast to wild-type GFP, which is not expressed at detectable levels in *C. albicans,* expression of the yEGFP was detectable both by fluorescence and by Western blotting, and showed brighter fluorescence in *Saccharomyces cerevisiae* than the wild-type protein. Efficiency of translation and transcription were also increased.

Plants exhibit specific problems in relation to GFP expression such as, low or unstable expression due to missplicing of the GFP mRNA [for example, in *Arabidopsis* (106, 107)] and interference in fluorescence detection by endogenous green pigmentation and chlorophyll fluorescence, as discussed previously. Rouwendal *et al.* (108) modified the codon usage of the wild-type *GFP* gene to enhance its expression in tobacco plants (*Nicotiana tabacum*). A synthetic *GFP* gene was created, increasing the frequency of codons with a C or G base at the third position from 32 to 60%. After comparing the expression of the synthetic gene with that of the wild-type gene in tobacco plants, it was found that the codon-modified gene increased the frequency of transgenic plants with high GFP expression.

Davis and Vierstra (109) incorporated amino acid substitutions into a version of a plant codon-optimized GFP to create brighter GFPs for use in higher plants. By site-directed mutagenesis they created a plant-optimized S65T derivative and a Y66H derivative, giving a BFP mutant. Into these derivatives they also incorporated three mutations that create a more soluble protein by improving protein folding. The spectra of both new fluorescent proteins were identical to their respective parent (S65T and Y66H) proteins and both proteins were found to be more soluble than the wild-type protein in *E. coli.* The new proteins were coexpressed in *Arabidopsis thaliana* seedlings and it was

possible to detect both blue and green fluorescence (using DAPI and FITC filters, respectively) in the same seedling. Fluorescence from the soluble plant BFP showed little background interference from the coexpressed GFP, suggesting that the two proteins are suitable for dual-labeling experiments. Cells expressing the soluble codon-optimized S65T GFP were significantly more fluorescent than cells expressing the parent codon-optimized version.

Finally, it is worth noting that the choice of promoter to drive GFP expression can be crucial to the sensitivity of the fluorescence assay. This is especially relevant for detection in plants as GFP fluorescence in green tissues, such as the leaf, is often totally masked by autofluorescence. For example, Kohler *et al.* (110) used a 35S35SAMV promoter (double constitutive 35S promoter) to be able to visualize expression of the plant codon-optimized GFP and the S65T GFP, whereas Hu and Cheng (111) used the single cauliflower mosaic virus 35S promoter to express GFP in tobacco plants and were unable to detect fluorescence. The reason for the discrepancy in these two studies is largely the promoters used. The 35S promoter is about 20 times less active than the 35S35SAMV promoter (112), resulting in the much lower sensitivity seen by Hu and Cheng (111).

However, overexpression of GFP can result in loss of definition of the fluorescent signal in microscopy and can also be toxic to the host cells. For example, Liu *et al.* (113) demonstrated the induction of apoptosis (programmed cell death) by three mutant GFPs in four mammalian cell lines. GFP toxicity has also been noted in plants (100, 108), particularly *A. thaliana* (107), although Niwa and co-workers (79) have since demonstrated nontoxic high-level expression of a synthetic, codon-optimized GFP in *Arabidopsis*.

CONCLUSIONS

This Review has indicated the main sources of autofluorescence and highlighted a wide range of varied techniques for removing interfering autofluorescence from measurements of GFP. Those methods that are likely to be the most appealing are those which do not negate the exquisite advantages of using GFP in the first place, namely the ability for nondestructive, *in vivo,* expression and measurement. These are noninvasive methods such as dual wavelength differential fluorescence correction, fluorescence polarization, and time-resolved techniques, all of which rely on different inherent spectroscopic properties of GFP and the autofluorescent species.

As the number of biological applications of GFP continues to increase, along with the commercial potential, so the drive exists for developing ever improved genetically altered derivatives of GFP. These will be significantly brighter, fluoresce at longer wavelengths, and be more specifically optimized for particular species and applications. With these improvements it is likely that in many cases the new generation of GFPs will outshine the autofluorescence, which will become much less of a problem. In turn, the use of brighter fluorescent markers will allow the use of less expensive instrumentation for both the excitation, quantification and imaging of GFP. For example, the use of light-emitting diodes, simple cutoff filters, and less sensitive photodetectors, will further increase the appeal of this truly remarkable fluorophore.

ACKNOWLEDGMENTS

The authors acknowledge Drs. R. M Walmsley, M. G Barker, and J. E. Prest for their assistance in the final revisions and corrections to the manuscript. The authors also thank Clontech Laboratories, Inc. for the generous provision of the spectra of GFP derivatives comprising Fig. 8. A. W. Knight and N. Billinton are supported by a grant from Gentronix Ltd. (www.gentronix.co.uk).

REFERENCES

1. Fellner, M. J. (1976) *Arch. Dermatol.* **112,** 667–670.
2. Nokubo, M., Ohta, M., Kitani, K., and Zs.-Nagy, I. (1989) *Biochim. Biophys. Acta* **981,** 303–308.
3. Plautz, J. D., Day, R. N., Dailey, G. M., Welsh, S. B., Hall, J. C., Halpain, S., and Kay, S. A. (1996) *Gene* **173,** 83–87.
4. Margo, C. E., and Bombardier, T. (1985) *Surv. Ophthalmol.* **29,** 374–376.
5. Graham, A. R. (1983) *Am. J. Clin. Pathol.* **79,** 231–234.
6. Dellinger, M., Geze, M., Santus, R., Kohen, E., Kohen, C., Hirschberg, J. G., and Monti, M. (1998) *Biotechnol. Appl. Biochem.* **28,** 25–32.
7. van der Geest, A. H. M., and Petolino, J. F. (1998) *Plant Cell Rep.* **17,** 760–764.
8. Vallet, C., Chabbert, B., Czaninski, Y., and Monties, B. (1996) *Ann. Bot.* **78,** 625–632.
9. Metcalf, R. L. (1943) *Arch. Biochem.* **2,** 55–62.
10. Benson, R. C., Meyer, R. A., Zaruba, M. E., and McKhann, G. M. (1979) *J. Histochem. Cytochem.* **27,** 44–48.
11. Aubin, J. E. (1979) *J. Histochem. Cytochem.* **27,** 36–43.
12. van Duijn, C., Jr. (1954) *Br. J Microsc. Photomicrogr.* **10,** 1–6.
13. Galeotti, T., van Rossum, G. D., Mayer, D. H., and Chance, B. (1970) *Eur. J. Biochem.* **17,** 485–496.
14. Schneckenburger, H., Gessler, P., and Pavenstädt-Grupp, I. (1992) *J. Histochem. Cytochem.* **40,** 1573–1578.
15. Yin, D. Z. (1996) *Free Radical Biol. Med.* **21,** 871–888.
16. Harman, D. (1990) *in* Lipofuscin and Ceroid Pigments (Porta, E. A., Ed.), pp. 3–15, Plenum, New York.
17. Clokey, G. V., and Jacobson, L. A. (1986) *Mech. Ageing Dev.* **35,** 79–94.
18. Wolman, M. (1980) *in* Pathobiology Annual (Ioachim, H. L., Ed.), Vol. 10, pp. 253–267, Raven Press, New York.
19. Gao, G. X., Ollinger, K., and Brunk, U. T. (1994) *Free Radical Biol. Med.* **16,** 187–194.
20. Schnell, S. A., Staines, W. A., and Wessendorf, M. W. (1999) *J. Histochem. Cytochem.* **47,** 719–730.
21. Pongor, S., Ulrich, P. C., Bencsath, F. A., and Cerami, A. (1984) *Proc. Natl. Acad. Sci. USA* **81,** 2684–2688.

22. Chang, J. C. F., Ulrich, P. C., Bucala, R., and Cerami, A. (1985) *J. Biol. Chem.* **260,** 7970–7974.
23. Sady, C., Khosrof, S., and Nagaraj, R. (1995) *Biochem. Biophys. Res. Commun.* **214,** 793–797.
24. Abiko, T., Abiko, A., Ishiko, S., Takeda, M., Horiuchi, S., and Yoshida, A. (1999) *Exp. Eye Res.* **68,** 361–366.
25. Sell, D. R., Lapolla, A., Odetti, P., Fogarty, J., and Monnier, V. M. (1992) *Diabetes* **41,** 1286–1292.
26. Fitzmaurice, M., Bordagaray, J. O., Engelmann, G. L., Richards-Kortum, R., Kolubayev, T., Feld, M. S., Ratliff, N. B., and Kramer, J. R. (1989) *Am. Heart J.* **118,** 1028–1038.
27. Bissonnette, R., Zeng, H. S., McLean, D. I., Schreiber, W. E., Roscoe, D. L., and Lui, H. (1998) *J. Invest. Dermatol.* **111,** 586–591.
28. Matz, M. V., Fradkov, A. F., Labas, Y. A., Savitsky, A. P., Zaraisky, A. G., Markelov, M. L., and Lukyanov, S. A. (1999) *Nat. Biotechnol.* **17,** 969–973.
29. He, X. Q., Li, S. W., Hu, Y. X., and Lin, J. X. (1999) *Acta Bot. Sinica* **41,** 711–714.
30. Donaldson, L. A., Singh, A. P., Yoshinaga, A., and Takabe, K. (1999) *Can. J. Bot.* **77,** 41–50.
31. Gunning, B. E. S., and Schwartz, O. M. (1999) *Aust. J. Plant Physiol.* **26,** 695–708.
32. Sheen, J., Hwang, S. B., Niwa, Y., Kobayashi, H., and Galbraith, D. W. (1995) *Plant J.* **8,** 777–784.
33. Stewart, C. N., Jr. (1996) *Nat. Biotechnol.* **14,** 682.
34. Plautz, J. D., and Kay, S. A. (1999) *in* Green Fluorescent Proteins (Sullivan, K. F., and Kay, S. A., Eds.), 1st ed., pp. 283–291, Academic Press, San Diego.
35. Hazelrigg, T. (1998) *in* Green Fluorescent Protein: Proteins, Applications and Protocols (Chalfie, M., and Kain, S., Eds.), 1st ed., pp. 169–190, Wiley, New York.
36. Brand, A. (1995) *Trends Genet.* **11,** 324–325.
37. Udenfriend, S. (1969) Fluorescence Assay in Biology and Medicine (Horecker, B., Kaplan, N. O., Marmur, J., and Scheraga, H. A., Eds.), Vol. II, Academic Press, New York/London.
38. Kahana, J. A., and Silver, P. A. (1998) *in* Green Fluorescent Protein: Proteins, Applications and Protocols (Chalfie, M., and Kain, S., Eds.), 1st ed., pp. 139–152, Wiley, New York.
39. Zylka, M. J., and Schnapp, B. J. (1996) *BioTechniques* **21,** 220–226.
40. Randers-Eichhorn, L., Albano, C. R., Sipior, J., Bentley, W. E., and Rao, G. (1997) *Biotechnol. Bioeng.* **55,** 922–926.
41. Endow, S. A., and Piston, D. W. (1998) *in* Green Fluorescent Protein: Proteins, Applications and Protocols (Chalfie, M., and Kain, S., Eds.), 1st ed., pp. 320–356, Wiley, New York.
42. Steinkamp, J. A., and Stewart, C. C. (1986) *Cytometry* **7,** 566–574.
43. Roederer, M., and Murphy, R. F. (1986) *Cytometry* **7,** 558–565.
44. Knight, A. W., Goddard, N. J., Fielden, P. R., Barker, M. G., Billinton, N., and Walmsley, R. M. (1999) *Anal. Commun.* **36,** 113–117.
45. Knight, A. W., Goddard, N. J., Fielden, P. R., Gregson, A. L., Billinton, N., Barker, M. G., and Walmsley, R. M. (2000) *Analyst* **125,** 499–506.
46. Swaminathan, R., Hoang, C. P., and Verkman, A. S. (1997) *Biophys. J.* **72,** 1900–1907.
47. Billinton, N., Barker, M. G., Michel, C. E., Knight, A. W., Heyer, W. D., Goddard, N. J., Fielden, P. R., and Walmsley, R. M. (1998) *Biosensors Bioelectronics* **13,** 831–838.
48. Nagatani, N., Takumi, S., Tomiyama, M., Shimada, T., and Tamiya, E. (1997) *Plant Sci.* **124,** 49–56.
49. Niswender, K. D., Blackman, S. M., Rohde, L., Magnuson, M. A., and Piston, D. W. (1995) *J. Microsc.* **180,** 109–116.
50. Potter, S. M., Wang, C. M., Garrity, P. A., and Fraser, S. E. (1996) *Gene* **173,** 25–31.
51. Denk, W., and Svoboda, K. (1997) *Neuron* **18,** 351–357.
52. Pepperkok, R., Squire, A., Geley, S., and Bastiaens, P. I. H. (1999) *Curr. Biol.* **9,** 269–272.
53. Craig, D. B., Wong, J. C. Y., and Dovichi, N. J. (1997) *Biomed. Chromatogr.* **11,** 205–206.
54. Malek, A., and Khaledi, M. G. (1999) *Anal. Biochem.* **268,** 262–269.
55. Korf, G. M., Landers, J. P., and O'Kane, D. J. (1997) *Anal. Biochem.* **251,** 210–218.
56. Walmsley, R. M., Billinton, N., and Heyer, W. D. (1997) *Yeast* **13,** 1535–1545.
57. Sherman, F., Fink, G. R., and Hicks, J. B. (1986) Laboratory Course Manual for Methods in Yeast Genetics, Cold Spring Harbor Laboratory Press, Cold Spring Harbor, NY.
58. Walmsley, R. M., Gardner, D. C., and Oliver, S. G. (1983) *Mol. Gen. Genet.* **192,** 361–365.
59. Lissemore, J. L., Jankowski, J. T., Thomas, C. B., Mascotti, D. P., and deHaseth, P. L. (2000) *BioTechniques* **28,** 82–89.
60. Andersson, H., Baechi, T., Hoechl, M., and Richter, C. (1998) *J. Microsc.* **191,** 1–7.
61. Sewell, W. F., and Mroz, E. A. (1993) *Hearing Res.* **70,** 131–138.
62. Nokubo, M., Zs.-Nagy, I., Kitani, K., and Ohta, M. (1988) *Biochim. Biophys. Acta* **939,** 441–448.
63. Galland, P., and Senger, H. (1988) *J. Photochem. Photobiol. B Biol.* **1,** 277–294.
64. Bessey, O. A., Lowry, O. H., and Love, R. H. (1949) *J. Biol. Chem.* **180,** 755–769.
65. Chalfie, M., Tu, Y., Euskirchen, G., Ward, W. W., and Prasher, D. C. (1994) *Science* **263,** 802–805.
66. Ward, W. W. (1998) *in* Green Fluorescent Protein: Proteins, Applications and Protocols (Chalfie, M., and Kain, S., Eds.), 1st ed., pp. 45–75, Wiley, New York.
67. Carminati, J. L., and Stearns, T. (1999) *in* Green Fluorescent Proteins (Sullivan, K. F., and Kay, S. A., Eds.), 1st ed., p. 93, Academic Press, San Diego.
68. Ferrigno, P., and Silver, P. A. (1999) *in* Green Fluorescent Proteins (Sullivan, K. F., and Kay, S. A., Eds.), 1st ed., p. 110, Academic Press, San Diego.
69. Kavanagh, F., and Goodwin, R. H. (1949) *Arch. Biochem.* **20,** 315–324.
70. Mayeno, A. N., Hamann, K. J., and Gleich, G. J. (1992) *J. Leukocyte Biol.* **51,** 172–175.
71. Patterson, G. H., Knobel, S. M., Sharif, W. D., Kain, S. R., and Piston, D. W. (1997) *Biophys. J.* **73,** 2782–2790.
72. Ward, W. W., and Bokman, S. H. (1982) *Biochemistry* **21,** 4535–4540.
73. Johnson, A. W., and Kolodner, R. D. (1991) *J. Biol. Chem.* **266,** 14046–14054.
74. Deschamps, J. R., Miller, C. E., and Ward, K. B. (1995) *Protein Expression Purif.* **6,** 555–558.
75. Nordstrom, T., Senkas, A., Eriksson, S., Pontynen, N., Nordstrom, E., and Lindqvist, C. (1999) *J. Biotechnol.* **69,** 125–133.
76. Yakhnin, A. V., Vinokurov, L. M., Surin, A. K., and Alakhov, Y. B. (1998) *Protein Expression Purif.* **14,** 382–386.
77. Finger, F. P., Hughes, T. E., and Novick, P. (1998) *Cell* **92,** 559–571.

78. Ellenberg, J., and Lippincott-Schwartz, J. (1999) *Methods* **19,** 362–372.
79. Niwa, Y., Hirano, T., Yoshimoto, K., Shimizu, M., and Kobayashi, H. (1999) *Plant J.* **18,** 455–463.
80. Simonova, M., Weissleder, R., Sergeyev, N., Vilissova, N., and Bogdanov, A., Jr. (1999) *Biochem. Biophys. Res. Commun.* **262,** 638–642.
81. Margolin, W. (2000) *Methods* **20,** 62–72.
82. Levitan, E. S. (1998) *Methods* **16,** 182–187.
83. Kunze, I., Hensel, G., Adler, K., Bernard, J., Neubohn, B., Nilsson, C., Stoltenburg, R., Kohlwein, S. D., and Kunze, G. (1999) *Biochim. Biophys. Acta* **1410,** 287–298.
84. Gerdes, H. H., and Rudolf, R. (1999) *Protoplasma* **209,** 1–8.
85. Laukkanen, M. L., Oker-Blom, C., and Keinanen, K. (1996) *Biochem. Biophys. Res. Commun.* **226,** 755–761.
86. Mosiman, V. L., Patterson, B. K., Canterero, L., and Goolsby, C. L. (1997) *Cytometry* **30,** 151–156.
87. Endow, S. A. (1999) *in* Green Fluorescent Proteins (Sullivan, K. F., and Kay, S. A., Eds.), 1st ed., pp. 156–158, Academic Press, San Diego.
88. Cubitt, A. B., Heim, R., Adams, S. R., Boyd, A. E., Gross, L. A., and Tsien, R. Y. (1995) *Trends Biochem. Sci.* **20,** 448–455.
89. Chattoraj, M., King, B. A., Bublitz, G. U., and Boxer, S. G. (1996) *Proc. Natl. Acad. Sci. USA* **93,** 8362–8367.
90. Elowitz, M. B., Surette, M. G., Wolf, P. E., Stock, J., and Leibler, S. (1997) *Curr. Biol.* **7,** 809–812.
91. Gadella, T. W. J., Jr., van der Krogt, G. N. M., and Bisseling, T. (1999) *Trends Plant Sci.* **4,** 287–291.
92. Day, R. N. (1998) *Mol. Endocrinol.* **12,** 1410–1419.
93. Sagot, I., Bonneu, M., Balguerie, A., and Aigle, M. (1999) *FEBS Lett.* **447,** 53–57.
94. Prasher, D. C., Eckenrode, V. K., Ward, W. W., Prendergast, F. G., and Cormier, M. J. (1992) *Gene* **111,** 229–233.
95. Heim, R., Prasher, D. C., and Tsien, R. Y. (1994) *Proc. Natl. Acad. Sci. USA* **91,** 12501–12504.
96. Ormö, M., Cubitt, A. B., Kallio, K., Gross, L. A., Tsien, R. Y., and Remington, S. J. (1996) *Science* **273,** 1392–1395.
97. Heim, R., Cubitt, A. B., and Tsien, R. Y. (1995) *Nature* **373,** 663–664.
98. Cormack, B. P., Valdivia, R. H., and Falkow, S. (1996) *Gene* **173,** 33–38.
99. Zolotukhin, S., Potter, M., Hauswirth, W. W., Guy, J., and Muzyczka, N. (1996) *J. Virol.* **70,** 4646–4654.
100. Chiu, W. L., Niwa, Y., Zeng, W., Hirano, T., Kobayashi, H., and Sheen, J. (1996) *Curr. Biol.* **6,** 325–330.
101. Yang, T. T., Cheng, L. Z., and Kain, S. R. (1996) *Nucleic Acids Res.* **24,** 4592–4593.
102. Yang, T. T., Sinai, P., Green, G., Kitts, P. A., Chen, Y. T., Lybarger, L., Chervenak, R., Patterson, G. H., Piston, D. W., and Kain, S. R. (1998) *J. Biol. Chem.* **273,** 8212–8216.
103. Angres, B., and Green, G. (1999) CLONTECHniques, April (also, http://www.clontech.com/archive/APR99UPD/dual.html).
104. Miyawaki, A., Llopis, J., Heim, R., McCaffery, J. M., Adams, J. A., Ikura, M., and Tsien, R. Y. (1997) *Nature* **388,** 882–887.
105. Cormack, B. P., Bertram, G., Egerton, M., Gow, N. A. R., Falkow, S., and Brown, A. J. P. (1997) *Microbiology* **143,** 303–311.
106. Haseloff, J., and Amos, B. (1995) *Trends Genet.* **11,** 328–329.
107. Haseloff, J., Siemering, K. R., Prasher, D. C., and Hodge, S. (1997) *Proc. Natl. Acad. Sci. USA* **94,** 2122–2127.
108. Rouwendal, G. J. A., Mendes, O., Wolbert, E. J. H., and de Boer, A. D. (1997) *Plant Mol. Biol.* **33,** 989–999.
109. Davis, S. J., and Vierstra, R. D. (1998) *Plant Mol. Biol.* **36,** 521–528.
110. Kohler, R. H., Zipfel, W. R., Webb, W. W., and Hanson, M. R. (1997) *Plant J.* **11,** 613–621.
111. Hu, W., and Cheng, C. L. (1995) *FEBS Lett.* **369,** 331–334.
112. Datla, R. S. S., Bekkaoui, F., Hammerlindl, J. K., Pilate, G., Dunstan, D. I., and Crosby, W. L. (1993) *Plant Sci.* **94,** 139–149.
113. Liu, H. S., Jan, M. S., Chou, C. K., Chen, P. H., and Ke, N. J. (1999) *Biochem. Biophys. Res. Commun.* **260,** 712–717.
114. Kawada, T., Shin, W. S., Nakatsuru, T., Koizumi, A., Sakamoto, T., Nakajima, Y., Okai-Matsuo, M., Nakazawa, M., Sato, H., Ishikawa, T., and Toyo-Oka, T. (1999) *Biochem. Biophys. Res. Commun.* **259,** 408–413.
115. Dowson, J. H. (1982) *J. Microscopy* **128,** 261–270.
116. Yin, D., Yuan, X. M., and Brunk, U. T. (1995) *Mech. Ageing Dev.* **81,** 37–50.
117. Katz, M. L., Eldred, G. E., and Robison, W. G., Jr. (1987) *Mech. Ageing Dev.* **39,** 81–90.
118. Morise, H., Shimomura, O., Johnson, F. H., and Winant, J. (1974) *Biochemistry* **13,** 2656–2662.
119. Crameri, A., Whitehorn, E. A., Tate, E., and Stemmer, W. P. C. (1996) *Nat. Biotechnol.* **14,** 315–319.